UNIVERSITÄTSKLINIKUM HAMBURG-EPPENDORF

Institut für Neuroimmunologie und Multiple Sklerose

Prof. Dr. med. Manuel A. Friese

Die Robustheit der Sehleistung während der frühen Neurodegeneration des visuellen Systems in der Primär Progredienten Multiplen Sklerose

Dissertation

zur Erlangung des Grades eines Doktors der Medizin

an der Medizinischen Fakultät der Universität Hamburg.

vorgelegt von:

Lilija Gutmann

aus Charkow

Hamburg 2023

Angenommen von der

Medizinischen Fakultät der Universität Hamburg am: 15.10.2024

Veröffentlicht mit Genehmigung der

Medizinischen Fakultät der Universität Hamburg.

Prüfungsausschuss, der/die Vorsitzende: PD. Dr. Andrea Hassenstein

Prüfungsausschuss, zweite/r Gutachter/in: PD. Dr. Jan-Patrick Stellmann

Inhaltsverzeichnis

1. Publikation

Multiple sclerosis

Original research

Visual function resists early neurodegeneration in the visual system in primary progressive multiple sclerosis

Sina C Rosenkranz ,[1] Lilija Gutmann,[1] Arzu Ceylan Has Silemek,[1] Michael Dorr ,[2] Vivien Häußler ,[1] Margareta Lüpke,[1] Andrea Mönch,[1] Stefanie Reinhardt,[1] Jens Kuhle,[3,4] Penelope Tilsley,[5,6] Christoph Heesen ,[1] Manuel A Friese ,[1] Alexander Brandt,[7,8] Friedemann Paul,[7] Hanna Zimmermann,[7] Jan-Patrick Stellmann [1,5,6]

► Additional supplemental material is published online only. To view, please visit the journal online (http://dx.doi.org/10.1136/jnnp-2023-331183).

For numbered affiliations see end of article.

Correspondence to
Dr Jan-Patrick Stellmann, Aix-Marseille Université, CRMBM, CNRS UMR 7339, Marseille, France; jan-patrick.STELLMANN@univ-amu.fr

SCR and LG contributed equally.

Received 1 February 2023
Accepted 31 May 2023

To cite: Rosenkranz SC, Gutmann L, Has Silemek AC, *et al*. *J Neurol Neurosurg Psychiatry* Epub ahead of print: [*please include* Day Month Year]. doi:10.1136/jnnp-2023-331183

ABSTRACT

Background Neurodegeneration in multiple sclerosis (MS) affects the visual system but dynamics and pathomechanisms over several years especially in primary progressive MS (PPMS) are not fully understood.

Methods We assessed longitudinal changes in visual function, retinal neurodegeneration using optical coherence tomography, MRI and serum NfL (sNfL) levels in a prospective PPMS cohort and matched healthy controls. We investigated the changes over time, correlations between outcomes and with loss of visual function.

Results We followed 81 patients with PPMS (mean disease duration 5.9 years) over 2.7 years on average. Retinal nerve fibre layer thickness (RNFL) was reduced in comparison with controls (90.1 vs 97.8 µm; p<0.001). Visual function quantified by the area under the log contrast sensitivity function (AULCSF) remained stable over a continuous loss of RNFL (0.46 µm/year, 95% CI 0.10 to 0.82; p=0.015) up until a mean turning point of 91 µm from which the AULCSF deteriorated. Intereye RNFL asymmetry above 6 µm, suggestive of subclinical optic neuritis, occurred in 15 patients and was related to lower AULCSF but occurred also in 5 out of 44 controls. Patients with an AULCSF progression had a faster increase in Expanded Disability Status Scale (beta=0.17/year, p=0.043). sNfL levels were elevated in patients (12.2 pg/mL vs 8.0 pg/mL, p<0.001), but remained stable during follow-up (beta=−0.14 pg/mL/year, p=0.291) and were not associated with other outcomes.

Conclusion Whereas neurodegeneration in the anterior visual system is already present at onset, visual function is not impaired until a certain turning point. sNfL is not correlated with structural or functional impairment in the visual system.

WHAT IS ALREADY KNOWN ON THIS TOPIC

⇒ The visual system is of high interest to study neurodegeneration and repair in multiple sclerosis (MS). However, especially in primary progressive MS (PPMS), where neurodegeneration is more prominent, there is a lack of multimodal longitudinal studies integrating advanced visual system outcomes with other biomarkers such as serum neurofilament light chain (sNfL) levels.

WHAT THIS STUDY ADDS

⇒ Despite substantial and continuous subclinical visual system neurodegeneration in PPMS, it seems that visual impairment occurs only later in the disease course when neuronal loss crosses a certain threshold.

⇒ Interestingly, these changes are independent from elevated sNfL levels and moderately related to suspected subclinical optic neuritis. Advanced vision testing seems a promising prognostic marker in the clinical context as it was associated with disability progression in our cohort.

HOW THIS STUDY MIGHT AFFECT RESEARCH, PRACTICE OR POLICY

⇒ Multimodal assessment of the visual system including advanced computer adaptive testing of the area under the log contrast sensitivity function, optical coherence tomography, MRI and sNfL seems to be a patient-centred and scientifically valuable biomarker for future disease progression.

⇒ The evidence seems sufficient to provide a visual system framework for future phase II studies of neuroprotective agents in progressive MS and to develop this approach towards a personalised medicine.

INTRODUCTION

Accumulation of disability in multiple sclerosis (MS) is driven by chronic inflammation leading to gradual neurodegeneration. The latter is considered a hallmark of progressive MS, being especially pertinent in primary progressive MS (PPMS).[1] Understanding and counteracting neurodegenerative processes are major unmet needs for all MS subtypes and studies in PPMS may help to mechanistically understand them. However, it is still challenging to detect ongoing neurodegeneration as it often precedes clinical worsening. Longitudinal neurodegenerative biomarkers in MS which predict clinical progression are required. Visual system biomarkers might serve as an attractive source for longitudinal neurodegenerative biomarkers as they have a direct link to a specific clinical outcome and are easy to access without causing any harm to the patients.

Visual impairment is one of the most prevalent symptoms of MS, has high impact on quality of life[2] and is therapeutically approached.[3] Optical coherence tomography (OCT) can quantify integrity of the retinal nerve fibre layer (RNFL), the ganglion cell and inner plexiform layer (GCIPL) as well as the inner nuclear layer (INL) with high precision[4] and might also serve as a diagnostic tool in MS.[5] A reduction in RNFL and GCIPL has been observed in all subtypes of MS,[6] is rather independent from inflammatory disease activity and seems to be accelerated in progressive MS.[7] Retinal layer atrophy has been associated with high-contrast visual acuity (HCVA), low-contrast visual acuity, cortical atrophy[8] and cognitive impairment.[9] In progressive MS, reduced RNFL also seems to predict an increased risk of disability progression.[6] Thus, based on current knowledge, the visual system might be tightly associated with overall neurodegeneration in MS. While most of the studies analysing the visual system included individuals with relapsing-remitting MS (RRMS), there are only few reported studies on PPMS, often with low participant numbers.[6 10 11] Moreover, most previous studies focused on specific outcomes such as single retinal layers and their correlations. To characterise and understand the dynamics of neurodegenerative processes and their impact on disability, multimodal longitudinal analysis of the visual system especially in patients with progressive MS are urgently warranted.

Another biomarker that might represent neurodegeneration in MS is neurofilament light chain (NfL). NfL is one of the main components of the axonal cytoskeleton and axonal damage leads to a release into the cerebrospinal fluid and, to a lesser extent, into the serum where it can be measured with a single molecule array.[12] Many studies revealed that serum NfL (sNfL) levels are elevated in neurological diseases with neuroaxonal damage[13] and correlate with MRI activity and relapse rate in patients with MS.[14] Although several studies show that sNfL levels are associated with indicators of disease worsening such as optic neuritis[15] and brain atrophy,[16] it is still a matter of debate whether sNfL levels can predict long-term disability,[17] especially in patients with progressive MS, where inflammatory activity is barely present.[18] It has been shown that the presence of both an elevated sNfL level and a reduced GCIPL volume presents a stronger risk factor for future disease activity than the presence of each marker individually[19] and that elevated sNfL levels are associated with higher retinal neuroaxonal loss in patients with RRMS but not in patients with progressive MS.[20] However, associations between visual outcomes and sNfL levels in patients with progressive MS have not been explored, but are highly required to understand the MS disease-specific mechanisms in the visual system.[21]

We hypothesise that visual systems biomarkers could serve as a prediction tool for clinical worsening in patients with PPMS and are more precise than currently used predictive biomarkers as sNfL. In a large, longitudinal, observational cohort study on individuals with PPMS, we here report for the first time on a multimodal analysis of advanced visual function outcomes, OCT, MRI and sNFL levels in patients, together with a cross-sectional comparison with healthy controls.

MATERIALS AND METHODS

Participants

We included patients with PPMS from two observational cohorts between 2012 and 2018. Patients were either recruited at the MS outpatient clinic at the University Medical Centre Hamburg-Eppendorf (UKE), or at the NeuroCure Clinical Research Center, Charité - Universitätsmedizin Berlin, both Germany. Patients were eligible if they were diagnosed with PPMS according to the McDonald criteria 2010, had a maximum Expanded Disability Status Scale (EDSS) of 7.0 and were between 18 and 65 years old. Patients were excluded if they had major medical problems other than MS or a contraindication for MRI. Age-matched healthy controls were recruited at the UKE.

Procedures

Patients in Hamburg were evaluated annually with the EDSS, the Timed 25 Foot Walk Test (T25FWT), the Symbol Digit Modalities Test (SDMT) and the Nine Hole Peg Test (NHPT). Visual function was assessed on each eye separately using HCVA charts at 5 m and the complete contrast sensitivity function (CSF) measured by the quantitative CSF approach, which is a computerised test using a Bayesian adaptive method to assess the full CSF.[22] Several features were calculated from the CSF, including the area under the log CSF (AULCSF), the CSF acuity (the point estimate at full contrast) and contrast sensitivities at individual spatial frequencies (1.5, 3, 6, 12 and 18 cycles per degree (CPD)). Additionally, serum samples were collected at each visit. Healthy controls underwent a cross-sectional assessment including OCT, MRI and visual function without biosampling. Thus, an independent matched cohort of controls from the UKE biobank was used for comparison of sNfL levels. Patients in Berlin were assessed on an annual basis for up to 4 years and only HCVA, OCT and EDSS were examined.

OCT protocol and processing

OCT scans were performed with the Spectralis SD-OCT (Heidelberg Engineering, Heidelberg, Germany, pupils not dilated, eye tracking). For measurement of the peripapillary retinal nerve fibre layer thickness (RNFL), we used a ring scan around the optic nerve head (12°, 1536 A-scans, 16≤Automatic Real-Time (ART) averaging ≤100) using the device-internal segmentation module 6.0.14.0. Ring scans in Hamburg before 2015 were performed with a slightly higher diameter (~3.5 vs ~3.4 mm) and excluded from the RNFL thickness analyses. A macular volume scan (25°×30°, 61 B-scans, 768 A-scans per B-scan, 12≤ART≤15) quantified the retinal volume, GCIPL and the INL. Scans not meeting the OSCAR-IB consensus criteria[23] were excluded. The SAMIRIX pipeline[24] was used for intraretinal layer segmentation of the macula scans and volumes were extracted in a 3 mm diameter cylinder around the fovea. Layer segmentation was manually corrected by two experienced graders. Subclinical optic neuritis (sON) might be an important covariate and we defined an intraindividual RNFL thickness difference above 6 µm as suggestive for sON.

MRI protocol and processing

The MRI protocol was performed for all subjects in the same scanner (Siemens Skyra 3T) and included a three-dimensional T1-weighted magnetisation-prepared rapid acquisition with gradient echo (repetition time (TR)=1900 ms; echo time (TE)=2.46 ms; flip angle (FA)=9°; voxel size=0.9 mm^3), a T2-weighted sequence (TR=2800 ms; TE=18 ms; FA=160°; voxel size=0.5×0.5×3 mm^3), a diffusion tensor imaging scan (single-shell, 20 directions with non-collinear diffusion gradients (b=1000 s/mm^2) and a non-diffusion-weighted b0 image (1.9×1.9×2.0 mm). Diffusion data were only available in 42 patients. We used the FreeSurfer software (surfer.nmr.mgh.harvard.edu) for calculating brain and grey matter volume adjusted for total intracranial volume. The TractSeg pipeline[25] was used for segmentation of four white matter bundles associated with the processing of visual stimuli: optic radiation (OR), parieto-occipital-pontine tract (POPT), superior longitudinal

Table 1 Descriptive statistics

	Patients with PPMS (n=81)	Healthy controls vision (n=52)	Healthy controls sNfL (n=52)
Sex (female/male) n (%)	24/57 (29.7/70.3)	36/16 (69.2/30.8), p<0.001	25/27 (48.1/51.9), p=0.338
Age (years)	51.8 (36.0–69.0; SD 7.7)	50.2 (37.0–63.0; SD 7.6), p=0.244	50.2 (31.0–63.0; SD 7.2), p=0.025
Disease duration since diagnosis (years)	5.9 (0–20.2; SD 5.8)		
Centre (Hamburg/Berlin) (n)	64/17		
Follow-up (years)	2.7 (0–6.2; SD 1.7)		
Number of visits per patient			
Hamburg median (range)	4 (2–6)		
Berlin median (range)	3 (1–7)		
EDSS median (range)	3.5 (2.0–7.0)		
T25FWT (s)	5.9 (3.2–14.3; SD 2.2)		
NHPT (s)	25.9 (17.1–55.8; SD 7.7)		
SDMT correct answers	47.7 (17–80; SD 12.2)		
SDMT SD	−0.57 (−3.0–2.5; SD 1.24)		
Immunotherapies at baseline	Ocrelizumab: n=1 Mitoxantrone: n=1 β-Interferons: n=2		
New immunotherapies during follow-up	Rituximab/Ocrelizumab: n=1 after 1 year and n=3 after 4 years Cladribine: n=1 after 2 years		

Data are presented as means (range; SD) unless otherwise indicated. SD in comparison with a normative cohort of healthy individuals.
EDSS, Expanded Disability Status Scale; NHPT, Nine Hole Peg Test; PPMS, primary progressive MS; SDMT, Symbol Digit Modalities Test; T25FWT, Timed 25 Foot Walk Test.

fascicle II (SLF_II) and thalamo-occipital tract (T_OCC). We extracted mean diffusivity (MD) values averaged over each tract as a proxy for structural integrity.

sNfL measurement

Blood samples were collected in standard serum tubes, aliquoted and stored at −80°C. All samples were shipped at −80°C to the University Hospital Basel, Switzerland. sNfL levels were determined using the single-molecule array (Simoa; Quanterix, Lexington, Massachusetts, USA) assay.[26] We compared sNfL raw values in pg/mL from patients with PPMS with healthy controls. sNfL z-scores based on healthy controls were calculated as described previously.[26]

Statistical analysis

Descriptive statistics are presented as mean with SD, median with range or frequencies. Group differences and associations were evaluated with linear mixed effect (LME) models adjusted for repeated measurements and with random intercepts. All models were adjusted for age, sex, sON and, when examining RNFL thickness, the OCT protocol. To describe the rate of abnormality, we computed percentile ranks based on the normative data from the control cohorts. To determine putative collapsing points of structural outcomes for visual function, we used segmented regression adjusted for age, sex and sON. Finally, we defined groups of patients with any and without any loss of visual function (AULCSF) during follow-up and we used analysis of variance to investigate a time×group interaction adjusted for age, sex and sON for outcomes. P values <0.05 were considered statistically significant. All statistical analysis was performed with Statistics in R V.4.2.1.

RESULTS

Patients with PPMS show retinal neuroaxonal loss, high sNfL serum levels and impaired visual functions despite a lack of clinical optic neuritis

Eighty-one patients with PPMS and two control cohorts (each n=52) were enrolled in this study (table 1). Patients had a moderate disability level with a median EDSS of 3.5 (range 2.0–7.0). None of the participants reported a previous optic neuritis but 15 of 79 patients with values from both eyes (19%; 95%CI 11% to 29%) and 5 of 44 controls (11%; 95%CI 4% to 26%; p=0.399) had a RNFL difference between eyes above 6 µm which is suggestive of sON. The rate of sON in controls is compatible with the original cut-off definition based on the 95%CI of intereye differences from a previously published dataset including 31 healthy subjects.[5] Exploring density plots of eye differences for vision and OCT outcomes showed over all very similar distributions for patients and controls. Only retinal volume and RNFL showed a shift towards more asymmetry suggesting that a higher RNFL cut-off of 10 µm might be more suitable in PPMS (see online supplemental figure SF1). The mean follow-up time of patients was 2.7 years (SD 1.7; up to 6 years). RNFL asymmetry increased during the follow-up in the entire cohort (+0.4 µm/year, p=0.003) with a faster increase in those patients with an asymmetry at baseline (+1.0 µm/year, p=0.005).

First, we compared differences of visual system biomarkers and sNfL between patients and controls (table 2 and figure 1). Patients with PPMS had an impaired visual function with reduced AULCSF and CSF acuity, while HCVA differences did not reach significance (figure 1A-C). We noticed a tendency of higher spatial frequencies to be statistically significantly impaired despite a probable floor effect at very high spatial frequencies (figure 1D and CPD results in table 2). We observed lower thickness of RNFL and GCIPL in the OCT of patients with PPMS (figure 1E-H). Brain parenchymal fractions were not significantly reduced (figure 1I-J), while sNfL values were higher in patients with PPMS than in controls (figure 1K). Eyes suggestive for sON showed worse visual functioning (AULCSF and CSF acuity) and had lower retinal layer volumes (table 2). In PPMS, sON was also associated with increased MD values in the thalamo-occipital tracts, indicating a loss of structural tract integrity (figure 1L-O and table 2). However, sON was not related to sNfL values (table 2). Ageing was associated with a decrease in HCVA, total macula volume, GCIPL and INL thickness as well as in brain parenchymal fractions whereas NfL values increased with age (table 2, figure 1). Brain volume seemed to decrease faster in patients than in controls over the age range, what can be considered as a proxy of disease

Table 2 Comparison of vision, retinal layers and MRI parameters in patients with PPMS and healthy controls

	Patients with PPMS (n=81) 153 eyes	Healthy controls (n=52) 91 eyes				
	Cohort effect: estimate (95% CI)	Cohort effect: estimate (95% CI)	Effects	Estimate	95% CI	P value
Vision						
HCVA n=123 Observations=531	0.80 (0.75 to 0.85)	0.89 (0.80 to 0.98)	PPMS	−0.092	−0.197 to 0.012	0.084
			Age	−0.078	−0.134 to −0.022	**0.006***
			Male	0.034	−0.061 to 0.130	0.479
			sON	−0.026	−0.105 to 0.053	0.523
AULCSF n=104 Observations=430	1.17 (1.11 to 1.22)	1.26 (1.19 to 1.33)	PPMS	−0.096	−0.190 to −0.001	**0.047***
			Age	−0.002	−0.053 to 0.049	0.939
			Male	0.031	−0.059 to 0.121	0.502
			sON	−0.062	−0.117 to −0.007	**0.027***
CSF acuity n=104 Observations=430	1.29 (1.26 to 1.32)	1.37 (1.32 to 1.41)	PPMS	−0.075	−0.131 to −0.020	**0.007***
			Age	0.005	−0.025 to 0.035	0.754
			Male	0.007	−0.046 to 0.059	0.799
			sON	−0.045	−0.080 to −0.010	**0.012***
Contrast sensitivity at 1.5 CPD n=104 Observations=430	1.33 (1.29 to 1.37)	1.36 (1.31 to 1.41)	PPMS	−0.029	−0.099 to 0.042	0.428
			Age	−0.014	−0.053 to 0.024	0.469
			Male	0.028	−0.039 to 0.095	0.405
			sON	−0.038	−0.083 to 0.007	0.100
Contrast sensitivity at 3 CPD n=104 Observations=430	1.38 (1.33 to 1.43)	1.42 (1.37 to 1.49)	PPMS	−0.047	−0.128 to 0.033	0.249
			Age	−0.004	−0.048 to 0.039	0.844
			Male	0.022	−0.055 to 0.099	0.569
			sON	−0.042	−0.090 to 0.005	0.079
Contrast sensitivity at 6 CPD n=104 Observations=430	1.18 (1.12 to 1.24)	1.29 (1.21 to 1.37)	PPMS	−0.105	−0.209 to −0.000	**0.049***
			Age	0.011	−0.045 to 0.067	0.700
			Male	0.028	−0.072 to 0.127	0.581
			sON	−0.080	−0.140 to −0.020	**0.010***
Contrast sensitivity at 12 CPD n=104 Observations=430	0.64 (0.58 to 0.71)	0.78 (0.70 to 0.87)	PPMS	−0.143	−0.256 to −0.030	**0.014***
			Age	−0.006	−0.068 to 0.055	0.838
			Male	0.032	−0.075 to 0.139	0.562
			sON	−0.075	−0.152 to 0.003	0.058
Contrast sensitivity at 18 CPD n=104 Observations=430	0.24 (0.19 to 0.29)	0.36 (0.29 to 0.42)	PPMS	−0.114	−0.203 to −0.024	**0.013***
			Age	−0.020	−0.070 to 0.029	0.417
			Male	0.042	−0.043 to 0.126	0.332
			sON	−0.039	−0.104 to 0.025	0.232
OCT						
Peripapillary RNFL thickness (µm) n=110 Observations=402	90.6 (87.9 to 93.3)	97.3 (93.7 to 100.8)	PPMS	−6.647	−11.249 to −2.045	**0.005**
			Age	−2.183	−4.294 to −0.072	**0.043***
			Male	−2.015	−6.491 to 2.462	0.377
			sON	−8.590	−9.697 to −7.483	**<0.001***
Retinal volume (3 mm circle macula) (mm^3) n=98 Observations=436	2.35 (2.32 to 2.37)	2.38 (2.35 to 2.42)	PPMS	−0.039	−0.088 to 0.010	0.116
			Age	−0.040	−0.059 to −0.022	**<0.001***
			Male	0.036	−0.012 to 0.083	0.137
			sON	−0.028	−0.039 to −0.017	**<0.001***
GCIPL volume (3 mm circle macula) (mm^3) n=115 Observations=539	0.56 (0.54 to 0.57)	0.61 (0.59 to 0.64)	PPMS	−0.057	−0.086 to −0.027	**<0.001***
			Age	−0.012	−0.023 to −0.000	**0.041***
			Male	0.002	−0.026 to 0.030	0.902
			sON	−0.029	−0.036 to −0.022	**<0.001***
INL volume (3 mm circle macula) (mm^3) n=114 Observations=533	0.298 (0.293 to 0.303)	0.290 (0.282 to 0.297)	PPMS	0.008	−0.001 to 0.017	0.078
			Age	−0.007	−0.011 to −0.003	**0.001***
			Male	0.005	−0.004 to 0.013	0.273
			sON	0.005	0.002 to 0.008	**0.002***
sON: yes/no n (%)	15/64 (19.0/71.0%)	5/39 (11.4/88.6%)				
MRI						
Brain parenchymal fraction n=77 Observations=211	0.755 (0.746 to 0.763)	0.762 (0.746 to 0.777)	PPMS	−0.007	−0.025 to 0.012	0.468
			Age	−0.015	−0.022 to −0.008	**<0.001***
			Male	−0.001	−0.017 to 0.015	0.924
			sON	−0.001	−0.007 to 0.005	0.759

Continued

Table 2 Continued

	Patients with PPMS (n=81) 153 eyes	Healthy controls (n=52) 91 eyes				
	Cohort effect: estimate (95% CI)	Cohort effect: estimate (95% CI)	Effects	Estimate	95% CI	P value
Grey matter fraction n=77 Observations=211	0.419 (0.413 to 0.425)	0.409 (0.397 to 0.420)	PPMS	0.010	−0.003 to 0.023	0.119
			Age	−0.012	−0.017 to −0.007	**<0.001***
			Male	−0.008	−0.019 to 0.004	0.198
			sON	0.000	−0.004 to 0.004	0.865
Optic radiation (OR) (MD) n=44 Observations=87	0.791 (0.568 to 1.014)		Age	0.023	−0.016 to 0.061	0.245
			Male	−0.000	−0.074 to 0.074	0.996
			sON	0.028	−0.007 to 0.063	0.111
Parietooccipital pontine (POPT) (MD) n=39 Observations=73	0.735 (0.615 to 0.855)		Age	0.015	−0.006 to 0.036	0.155
			Male	0.008	−0.026 to 0.042	0.628
			sON	0.010	−0.019 to 0.039	0.507
Superior longitudinal fascicle II (SLF_II) (MD) n=46 Observations=98	0.700 (0.630 to 0.771)		Age	0.010	−0.002 to 0.022	0.112
			Male	−0.014	−0.036 to 0.009	0.234
			sON	0.007	−0.007 to 0.020	0.342
Thalamo-occipital (T_OCC) (MD) n=45 Observations=91	0.753 (0.524 to 0.981)		Age	0.031	−0.009 to 0.070	0.127
			Male	0.019	−0.054 to 0.092	0.603
			sON	0.050	0.010 to 0.091	**0.015***
sNfL						
sNfL (pg/mL) n=116 Observations=296	12.0 (11.0 to 13.0)	8.4 (6.9 to 9.9)†	PPMS	3.572	1.749 to 5.396	**<0.001***
			Age	1.942	0.785 to 3.099	**0.001***
			sON	1.041	−1.190 to 3.272	0.359
sNfL z-scores n=116 Observations=296	0.99 (0.75 to 1.24)	0.07 (−0.23 to 0.37)†	PPMS	0.923	0.535 to 1.312	**<0.001***
			sON	0.291	−0.039 to 0.621	0.083
sNfL percentiles n=116 Observations=296	74.3 (68.0 to 80.6)	53.2 (45.6 to 60.8)	PPMS	21.111	11.219 to 31.004	**<0.001***
			sON	5.833	−2.192 to 13.858	0.154

Overview of altered visual system outcomes in PPMS compared with healthy controls. Effects and their 95% CI are from linear mixed effects models with cohort, age, sex and sON as explanatory variables. For major brain tracts, data from controls were not available.
Brain and grey matter volumes are divided by the intracranial volume providing parenchymal fractions.
* indicates a p-value below 0.05.
†Independent healthy control cohort for sNfL comparison. Estimate of age effects reported as changes per decade.
AULCSF, area under the log contrast sensitivity function; CPD, cycles per degree; CSF, contrast sensitivity function; GCIPL, combined ganglion cell and inner plexiform layer; HCVA, high-contrast visual acuity; INL, inner nuclear layer; MD, mean diffusivity in 10^{-3}×mm^2/s; number of eyes, number of available RNFL values at baseline; OCT, optical coherence tomography; PPMS, primary progressive multiple sclerosis; RNFL, retinal nerve fibre layer; sNfL, serum neurofilament light chain; sON, subclinical optic neuritis.

duration in our cohort, but the interaction group×age did not reach significance (p=0.069).

Disease duration is not associated with visual function tests but with retinal neuronal layer loss

Next, we were interested how these parameters were related to disease duration (figure 2). We observed no significant association for the three visual function tests (figure 2A-C): HCVA (p=0.412), AULCSF (p=0.198) and CSF acuity (p=0.531). Absolute sNfL levels were not correlated with disease duration (beta=−0.15, 95% CI −0.42 to 0.11, p=0.291, figure 2D) but z-scores tended to decrease by 0.04/year (95% CI 0 to 0.08, p=0.050).

The RNFL thickness decreased with disease duration by 0.55 µm/year (95% CI 0.13 to 0.96; p=0.010; figure 2E), the retinal volume by 0.006 mm^3/year (95% CI 0.002 to 0.010; p=0.007; figure 2F) and the GCIPL volume by 0.004 mm^3/year (95% CI 0.001 to 0.007, p=0.002; figure 2G). The change in INL volume did not reach significance (p=0.700; figure 2H). MD increased in T_OCC by 0.06×10^{-3} mm^2/s for each year of disease duration (95% CI 0 to 0.12, p=0.037; figure 2J), whereas there was no association in the OR (p=0.124, figure 2I), POPT (p=0.369; figure 2K) and SLF_II (p=0.484; figure 2L). Due to the co-linearity between age and disease duration, we recomputed all models without age as a covariate. However, this did not change the results relevantly.

We visualised the loss in average percentile rank in comparison with controls in figure 2M. Only sNfL levels and INL volume were elevated at time of diagnosis while CSF acuity, RNFL thickness and GCIPL volume were already clearly reduced. GCIPL showed the most constant and clear decline. This indicates that a neuronal retinal layer loss precedes clinical visual functions by several years. Assuming a similar constant rate of GCIPL percentile rank loss (0.9%/year) before diagnosis (mean percentile rank 32.8), we estimated the time when our cohort was at the 50th percentile on average, that is, indistinguishable from controls. This silent onset of the disease was approximately 18 years before diagnosis (approximately 20 years based on RNFL thickness loss).

Loss of visual function presents at low retinal thickness values

Next, we investigated how neurodegeneration of the retina and visual tracts determines visual function. Figure 3 shows that visual function tests are stable or decrease very little up to a certain point of structural integrity loss after which there was a functional decrease associated with further neurodegeneration. Segmented regression determined these turning points of AULCSF stability at a RNFL thickness of 90.6 µm (figure 3A, 95% CI 84.9 to 96.3, p<0.001), and a GCIPL volume of 0.43 mm³ (figure 3B, 95% CI 0.40 to 0.46, p<0.001). AULCSF covering the whole spectrum of contrasts and spatial frequencies seemed to decline faster (standardised beta=0.89, p=0.010) than high-contrast outcomes

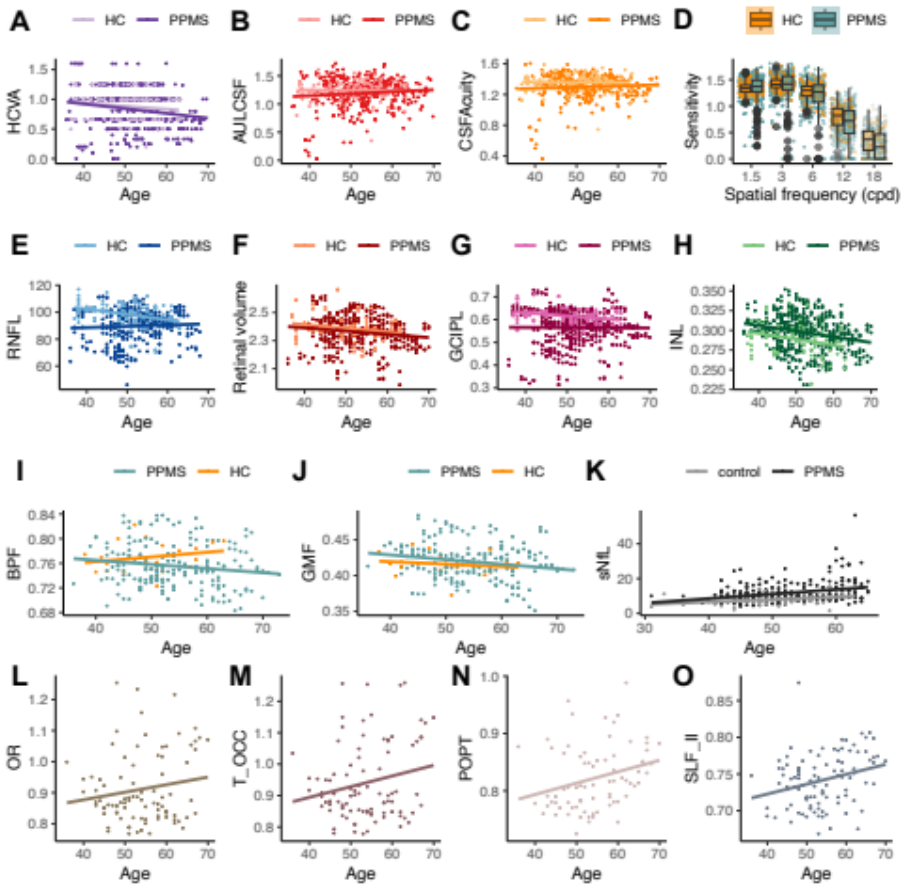

Figure 1 Vision, retinal layers, brain volumes and tracts in PPMS and HC. Dot plots with linear regression estimates (HC) illustrate age-corrected differences between the groups and a putative different dynamic between the group—as for example for BPF, which remains rather stable in controls between 40 and 60 years of age while there is a decrease in PPMS widening the gap between patient and controls at higher age. Figures are for illustrative purposes only and include all available data, that is, recurrent assessments for patients. For estimates and statistics, please refer to table 2 with linear mixed effects models results adjusting for age, sex and intraindividual correlations. Visual function tests (A–C), box plots illustrating differences in contrast sensitivity at different spatial frequencies between patients and controls (D), retinal layers (E–H), BPF (I), GMF (J), absolute sNfL levels in pg/mL (K) and tracts in the visual system (L–O). Mean diffusivity values for tracts (L–O) were only available from a subset (n=42) of patients. AULCSF, area under the log contrast sensitivity function; BPF, brain parenchymal fraction; CPD, cycles per degree; CSF, contrast sensitivity function; GCIPL, combined ganglion cell and inner plexiform layer; GMF, grey matter fraction; HC, healthy controls; HCVA, high-contrast visual acuity; INL, inner nuclear layer; OR, optic radiation; POPT, parieto-occipital-pontine tract; PPMS, primary progressive MS; RNFL, retinal nerve fibre layer; sNfL, serum neurofilament light chain; SLF_II, superior longitudinal fascicle II; T_OCC, thalamo-occipital tract;

(HCVA: standardised beta=0.39, p=0.001and CSF acuity: standardised beta=0.79, p<0.001). However, turning points for HCVA (RNFL: 92.1 µm, GCIPL: 0.41 mm^3) and CSF acuity (RNFL: 91.7 µm, GCIPL: 0.43 mm^3) were similar as for AULCSF. Out of the tracts, SLF_II (figure 3C) showed an accelerated functional loss above an MD threshold of 0.76 $10^{-3}\times mm^2/s$ (95%CI 0.74 to 0.78, p<0.001) for AULCSF. Only a very high borderline MD value indicated a functional loss in the T_OCC (figure 3D, 1.25 $10^3\times mm^2/s$, 95%CI 0.74 to 0.78, p<0.001), whereas OR and POPT showed no turning point. We found no cut-off value associated with sNfL z-scores. Associations between all outcomes are reported in detail in the supplemental material (online supplemental figure SF2, SF3 and table ST1).

AULCSF could serve as a prognostic tool for retinal thinning

As AULCSF seemed a more sensitive outcome to monitor visual function than HCVA and CSF acuity, we analysed whether other outcomes differed also between patients with a decline in AULCSF (individual beta-coefficient AULCSF over time <0, n=25) or without (n=26). Patients with an AULCSF progression showed a decrease in HCVA (beta=−0.09/year, p=0.005) and CSF acuity (beta=−0.03/year, p=0.007). The change in sNfL was similar in both groups (p=0.378). EDSS increased faster in patients with AULCSF progression (beta=0.17/year, p=0.043), while NHPT (p=0.939), T25FWT (p=0.172) and SDMT (p=0.790) dynamics did not differ between groups. The loss in RNFL (p=0.666) and retinal volume (p=0.523) did not differ between the groups. GCIPL decreased less in progressors than in stable patients (beta=0.004 mm^3/year, p=0.028) while INL volume remained stable in both groups (p=0.611). Changes in MD values from tracts did not differ between groups.

DISCUSSION

Our study revealed the predictive potential of visual system biomarkers for clinical worsening in PPMS. We detected a temporarily preserved visual function despite an early and ongoing

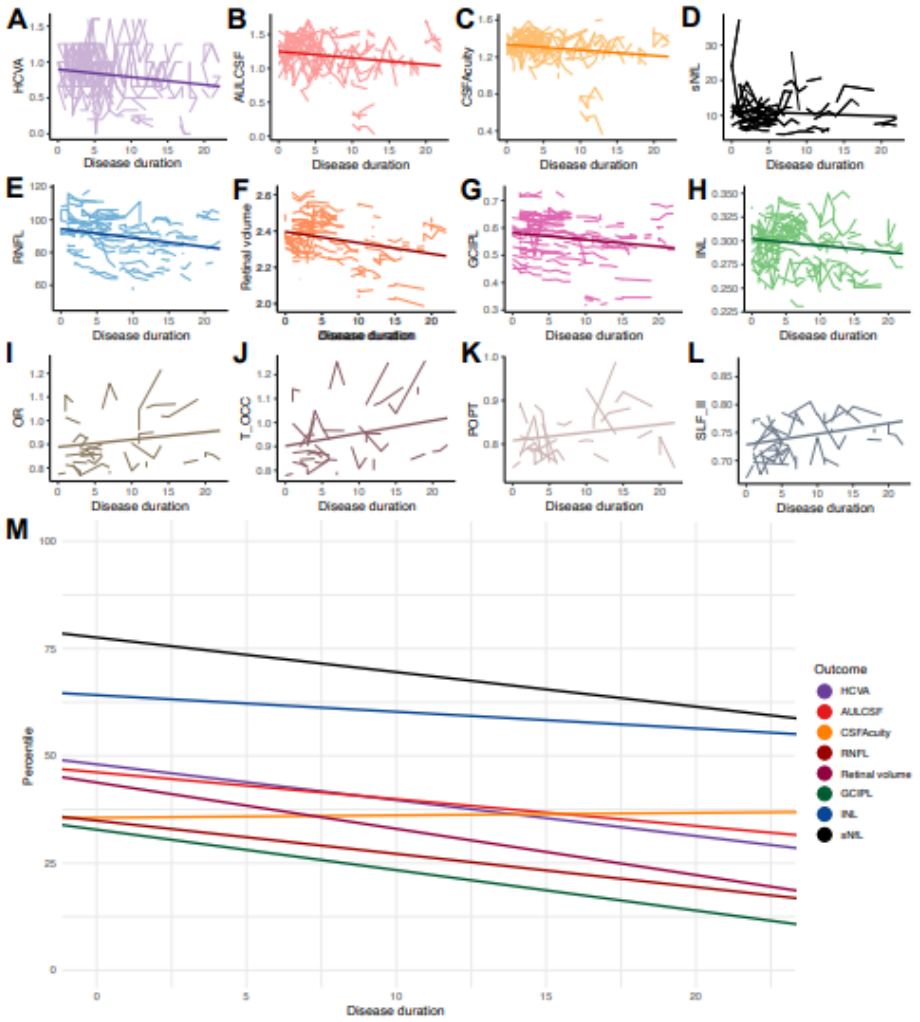

Figure 2 Changes in vision, sNfL levels, retinal layers and tracts over the disease course. Disease duration and outcomes: line plots for each patient or patients' eye with linear regression estimates for visual outcomes (A–C), absolute sNfL in pg/mL (D), retinal layers (E–H) and tracts in the visual system (I–L). Mean diffusivity values for tracts are only available for a subset of patients (n=42). Age-adjusted percentile ranks during the disease (M). Intercepts and slopes estimated with linear mixed effects regression (LMER). sNfL percentile ranks are based on the external normative cohort, other percentile ranks were computed in comparison with the healthy control cohort. Diffusion data could not be included in panel M due to the lack of reference data for percentile rank computation. HCVA, high-contrast visual acuity; AULCSF, area under the log contrast sensitivity function; CSF, contrast sensitivity function; RNFL, retinal nerve fibre layer; GCIPL, combined ganglion cell and inner plexiform layer; INL, inner nuclear layer; sNfL, serum neurofilament light chain; OR, optic radiation; T_OCC, thalamo-occipital tract; POPT, parieto-occipital-pontine tract; SLF_II, superior longitudinal fascicle II.

reduction of visual structural integrity in PPMS. Importantly, retinal neurodegeneration and active neuronal loss as indicated by high sNfL levels at the diagnosis of the disease support a preclinical neurodegeneration over several years.

Our large, multidimensional and longitudinal dataset confirmed cross-sectional observations that patients with PPMS have a significantly lower RNFL thickness, GCIPL volume and a trend towards a lower retinal volume when compared with healthy controls.[7] Compared with a younger cohort of 333 RRMS with a comparable disease duration below 10 years, RNFL thickness in our PPMS cohort of ~91 µm was more similar to patients without a history of ON (~92 µm) than to patients with a history of ON (~83 µm).[27] Here, every year of disease duration was associated with a RNFL thickness loss of approximately 0.55 µm/year which is rather similar to an ON independent rate of RNFL loss in the same RRMS cohort of 1.76 µm over 36 months or in other cohorts of 1.1 µm over 2 years.[27 28] Thus, continuous RNFL thickness loss in RRMS and PPMS seems very similar if independent from inflammatory ON activity, hence, it seems to represent rather ongoing neurodegeneration than acute inflammation. This conclusion might also explain why we did not observe an INL increase, which has previously been reported as a surrogate of inflammation in MS.[29] Moreover, our results underline that the association between retinal damage and visual function is not linear. We were able to determine turning points, for example, once RNFL thickness falls below 92.1 µm, retinal neurodegeneration begins to translate into faster, progressive visual function impairment as defined by the AULCSF. This is much higher than previously reported turning points of 60 µm for MS and other neuroinflammatory diseases using standard visual acuity charts.[30] Persisting high-contrast visual impairment after ON was previously only observed below a threshold of 75 µm RNFL thickness.[31] Interestingly, sON—as defined by the recently promoted 6 µm intereye difference

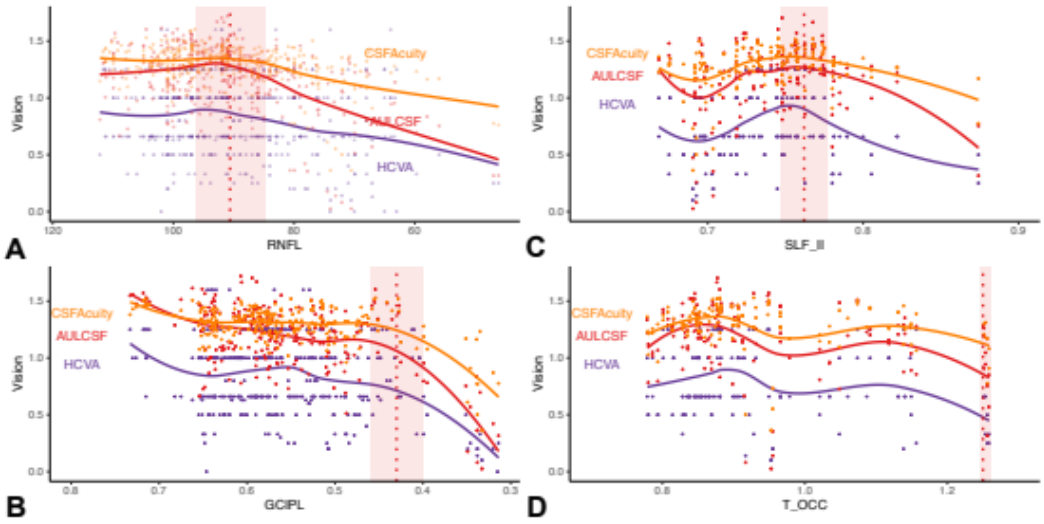

Figure 3 Association between structure and function in the visual system. Significant associations between visual functional tests (raw values for HCVA, AULCSF and CSF acuity on the y-axis), retinal integrity and optic tracts: optical coherence tomography outcomes on the left panels: (A) RNFL thickness and (B) GCIPL volume. The x-axis is inverted for retinal layers so that the thickness decreases from left to right, that is, with disease progression. Average mean diffusivity in tracts is displayed on the right panels for (C) SLF_II and (D) T_OCC. Dot plots of individual patient data are shown with smooth lines produced from local regression estimates (locally estimated scatterplot smoothing -LOESS). Red dotted line indicates the estimated turning point from segmented regression (the shaded area indicates the 95% CI). HCVA, high-contrast visual acuity; AULCSF, area under the log contrast sensitivity function; CSF, contrast sensitivity function; RNFL, retinal nerve fibre layer; GCIPL, combined ganglion cell and inner plexiform layer; T_OCC, thalamo-occipital tract; SLF_II, superior longitudinal fascicle II.

cut-off—was present in 1 out of 5 patients in our cohort and 1 out of 10 healthy controls. Given the expected rate of zero optic neuritis in both groups, the current definition seems not sufficiently sensitive and specific in our cohort. Our analysis revealed that a higher cut-off of around 10 µm might be more suitable, but this needs further investigations. In addition, it might be interesting to also study the longitudinal dynamic of intereye asymmetry, for RNFL and for other outcomes. However, the 6 µm sON definition showed a moderate association with CSF outcomes but had no relevant association with other outcomes in our cohort. This observation might underline the hypothesis that PPMS has a rather diffuse, sometimes asymmetric, neurodegenerative pathophysiology with a less focal lesioning aspect than RRMS. Moreover, asymmetry in PPMS might be less driven by silent optic neuritis but through imbalanced brain atrophy that translates via retrograde trans-synaptic degeneration from non-primary visual areas into the retina.[32] Our findings support the robustness of the visual system against neuronal damage in PPMS, which might be partially explained by functional reorganisation of information processing beyond primary visual areas and consecutive structural reorganisation.[33] The long preclinical phase despite proven substantial retinal damage in PPMS might thus hint towards a more resilient brain network architecture or physiology in comparison with other disease courses.

We found a distinct association between atrophy of the RNFL, GCIPL and retinal volume and a worsening of the vision parameters but no association between INL and clinical outcomes. Assessments using the complete CSF detected mild visual impairment earlier in the disease course than standard HCVA. The higher sensitivity of low-contrast visual acuity has been reported before, could be confirmed here by analysing different features derived from the CSF estimate and its relevance is underlined by better correlation with important health dimensions like participation or activities of daily living.[34] Despite the similarity of a pronounced impairment of low-contrast vision in RRMS and PPMS, reference data comparing contrast sensitivity and retinal integrity are lacking. Moreover, our analyses provide further evidence for trans-synaptic and downstream degeneration and its link to higher order functions.[35 36] Here, advanced anterior visual system impairment correlated with increased diffusivity, a sensitive marker of neuronal tract integrity, which links vision to other functional systems, namely a cognitive task measuring information processing.[37]

When investigating progression and outcome dynamics, we observed a more complex picture. In patients with a stable AULCSF over the disease course, the reduction of GCIPL volume was higher than in patients with AULCSF progression. This might be explained by the robustness of visual functioning against structural damage, already mentioned and discussed above. However, AULCSF progressors also had a faster increase in EDSS. Overall, our findings underline the heterogeneity of MS disability patterns in PPMS, the need for a precise disability assessment on an individual level and the advantage of multimodal studies.

In comparison with most other studies, we were able to evaluate the association of these changes with disability outcomes, MRI parameters and the levels of sNfL in a longitudinal setting. Over up to 5 years, we observed a homogeneous and constant thinning of retinal nerve layers and elevation of sNfL levels, indicating a rather constant rate of neurodegeneration in our cohort. Here, we did not observe a strong association between retinal atrophy and sNfL. Larger longitudinal datasets in PPMS might allow advanced modelling of associations including other disease characteristics and confounders of NfL levels like overall disability, lesions, spinal cord atrophy or body mass index. The highest sNfL values were detected at the beginning of the disease, followed by high and stable sNfL levels during follow-up. As sNfL concentrations increase with age,[38] we used z-scores which reflect the deviation to a control cohort.[39] Current studies in multiple sclerosis show a strong association

of sNfL with inflammatory activity in MS, while the increase specific to disease progression appears more subtle.[17 40–43] Many studies have shown associations between sNfL levels and clinical outcomes,[40 42 44] and it was also shown that NfL levels in the cerebrospinal fluid at the onset of optic neuritis predict low-contrast visual acuity, RNFL and GCIPL at follow-up.[15] Here, we could not detect any association between visual outcomes and sNfL levels, which might be explained by the presence of sNfL derived from neuronal damage outside of the visual system introducing variability. Moreover, sNfL levels did not differ between patients with stable or unstable AULCSF during the disease. However, follow-up studies including more patients with a longer disease duration are needed.

Our study has several limitations. Despite our cohort being rather large, understanding disease mechanisms in a pathology that acts over decades remains restricted. We also aimed to correlate the interaction between structure and function, but informative outcomes such as visual evoked potentials and functional MRI were not included in the design of the study. These would have allowed the determination of functional integrity and functional compensation, putative important mediators between structural damage and real-life performance. The lack of diffusion imaging in controls made a comparison of downstream structural connectivity of important brain tracts impossible. Also, the lack of longitudinal data for controls restricts the interpretability of longitudinal data in PPMS as normal ageing effects are not robustly captured in the cross-sectional comparison. Finally, our analyses are possibly limited by a variability and potential bias introduced by combining different datasets from two centres with two different control cohorts for sNfL and visual system.

In summary, we identified that visual function in people with PPMS is rather robust against neurodegeneration of retinal layers which is already present at the beginning of the disease. Interestingly, sNfL levels were not associated with visual function or thinning of retinal layers, while OCT and AULCSF could prove their usefulness in detecting neurodegeneration. The easy and highly precise multimodal assessment of its integrity might allow a personalised disease surveillance, prognosis and monitoring of putative neuroregenerative treatments in the future.

Author affiliations
[1]Institut für Neuroimmunologie und Multiple Sklerose (INIMS), Universitätsklinikum Hamburg-Eppendorf (UKE), Hamburg, Germany
[2]Adaptive Sensory Technology, Lübeck, Germany
[3]Multiple Sclerosis Centre and Research Center for Clinical Neuroimmunology and Neuroscience (RC2NB), Departments of Biomedicine and Clinical Research, University Hospital and University of Basel, Basel, Switzerland
[4]Department of Neurology, University Hospital and University of Basel, Basel, Switzerland
[5]CEMEREM, APHM, Hôpital de la Timone, Marseille, France
[6]CRMBM, Aix Marseille Univ, CNRS, Marseille, France
[7]Experimental and Clinical Research Center, Max Delbrück Center for Molecular Medicine and Charité - Universitätsmedizin Berlin, Corporate Member of Freie Universität Berlin and Humboldt-Universität zu Berlin, Berlin, Germany
[8]Department of Neurology, University of California Irvine, Irvine, California, USA

Twitter Sina C Rosenkranz @RosenkranzSina, Jens Kuhle @JensKuhle and Manuel A Friese @ManuelFriese; @inims_hamburg

Acknowledgements We thank all colleagues of the INIMS biobank.

Contributors SCR: conceptualisation, methodology, writing—original draft; LG: conceptualisation, methodology, formal analysis, writing—original draft; ACHS: formal analysis, writing—review and editing; MD: methodology, formal analysis, writing—review and editing; VH: investigation, writing—review and editing; ML: investigation, formal analysis, writing—review and editing; AM: investigation, writing—review and editing; SR: investigation, writing—review and editing; JK: methodology, formal analysis, writing—review and editing; PT: formal analysis, writing—review and editing; CH: conceptualisation, writing—review and editing; MAF: writing—review and editing; AB: conceptualisation, writing—review and editing; FP: conceptualisation, writing—review and editing; HZ: conceptualisation, methodology, writing—review and editing; J-PS: conceptualisation, methodology, formal analysis, visualisation, writing—original draft. J-PS accepts full responsibility for the conduct of the study, had access to the data, and controlled the decision to publish.

Funding Initial setup by unrestricted grants from Novartis and MerckSerono. SCR is funded by the Hertie Network of Excellence in Clinical Neuroscience of the Gemeinnützige Hertie Stiftung and by the Bundesministerium für Bildung und Forschung (Funding reference number 01EO2106).

Competing interests MD has financial and intellectual property interests in and holds employment by Adaptive Sensory Technology. MAF has received honoraria as speaker and for consultation from Biogen, Lundbeck, Merck KGaA, Novartis and Roche. His research is funded by the Bundesministerium für Bildung und Forschung (BMBF), Deutsche Forschungsgemeinschaft (DFG), Landesforschungsförderung Hamburg, Gemeinnützige Hertie-Stiftung, Else Kröner-Fresenius-Stiftung, Fritz Thyssen-Stiftung, Werner Otto-Stiftung and Deutsche Multiple Sklerose-Gesellschaft. HZ received speaking honoraria from Bayer Healthcare and Novartis and research grants from Novartis.

Patient consent for publication Not applicable.

Ethics approval The study was approved by the local ethics committee (Ethical Committee of the Board of Physicians Hamburg, PV4455, PV3961 and PV5557, Ethical Committee of the Charité, EA1/163/12). Participants gave informed consent to participate in the study before taking part.

Provenance and peer review Not commissioned; externally peer reviewed.

Data availability statement Data are available on reasonable request.

Author note Recent work in several fields of science has identified a bias in citation practices such that papers from women and other minority scholars are undercited relative to the number of such papers in the field. Here, we sought to proactively consider choosing references that reflect the diversity of the field in thought, form of contribution, gender, race, ethnicity and other factors. Using the CleanBib approach (https://github.com/dalejn/cleanBib), we obtained first the predicted gender of the first and last author of each reference by using databases that store the probability of a first name being carried by a woman. By this measure and excluding self-citations to the first and last authors of our current paper, our references contain 12.82% woman (first)/woman (last), 15.38% man/woman, 12.2% woman/man and 59.6% man/man. This method is limited in that (a) names, pronouns and social media profiles used to construct the databases may not, in every case, be indicative of gender identity and (b) it cannot account for intersex, non-binary or transgender people. Second, we obtained predicted racial/ethnic category of the first and last author of each reference by databases that store the probability of a first and last name being carried by an author of colour. By this measure (and excluding self-citations), our references contain 11.34% author of colour (first)/author of colour (last), 14.92% white author/author of colour, 23.26% author of colour/white author and 50.48% white author/white author. This method is limited in that (a) names and Florida Voter Data to make the predictions may not be indicative of racial/ethnic identity and (b) it cannot account for Indigenous and mixed-race authors, or those who may face differential biases due to the ambiguous racialisation or ethnicisation of their names. See also supplemental material for more extensive information about our citations. We look forward to future work that could help us to better understand how to support equitable practices in science.

ORCID iDs
Sina C Rosenkranz http://orcid.org/0000-0002-5228-4266
Michael Dorr http://orcid.org/0000-0002-7879-7908
Vivien Häußler http://orcid.org/0000-0002-7787-7391
Christoph Heesen http://orcid.org/0000-0001-8131-9467
Manuel A Friese http://orcid.org/0000-0001-6380-2420
Jan-Patrick Stellmann http://orcid.org/0000-0003-2565-2833

REFERENCES

1 Faissner S, Plemel JR, Gold R, *et al*. Progressive multiple sclerosis: from pathophysiology to therapeutic strategies. *Nat Rev Drug Discov* 2019;18:905–22.

2 Balcer LJ, Miller DH, Reingold SC, *et al*. Vision and vision-related outcome measures in multiple sclerosis. *Brain* 2015;138(Pt 1):11–27.
3 Lagrèze WA, Küchlin S, Ihorst G, *et al*. Safety and efficacy of erythropoietin for the treatment of patients with optic neuritis (TONE): a randomised, double-blind, Multicentre, placebo-controlled study. *Lancet Neurol* 2021;20:991–1000.
4 Petzold A, Balcer LJ, Calabresi PA, *et al*. Retinal layer Segmentation in multiple sclerosis: a systematic review and meta-analysis. *Lancet Neurol* 2017;16:797–812.
5 Petzold A, Chua SYL, Khawaja AP, *et al*. Retinal asymmetry in multiple sclerosis. *Brain* 2021;144:224–35.
6 Martínez-Lapiscina EH, Arnow S, Wilson JA, *et al*. Retinal thickness measured with optical coherence tomography and risk of disability worsening in multiple sclerosis: a cohort study. *Lancet Neurol* 2016;15:574–84.
7 Sotirchos ES, Gonzalez Caldito N, Filippatou A, *et al*. Progressive multiple sclerosis is associated with faster and specific retinal layer atrophy. *Ann Neurol* 2020;87:885–96.
8 Saidha S, Sotirchos ES, Oh J, *et al*. Relationships between retinal axonal and neuronal measures and global central nervous system pathology in multiple sclerosis. *JAMA Neurol* 2013;70:34–43.
9 Ko F, Muthy ZA, Gallacher J, *et al*. Association of retinal nerve fiber layer thinning with current and future cognitive decline: A study using optical coherence tomography. *JAMA Neurol* 2018;75:1198–205.
10 Pisa M, Ratti F, Vabanesi M, *et al*. Subclinical neurodegeneration in multiple sclerosis and Neuromyelitis Optica spectrum disorder revealed by optical coherence tomography. *Mult Scler* 2020;26:1197–206.
11 Klumbies K, Rust R, Dörr J, *et al*. Retinal thickness analysis in Progressive multiple sclerosis patients treated with Epigallocatechin Gallate: optical coherence tomography results from the SUPREMES study. *Front Neurol* 2021.
12 Kuhle J, Barro C, Andreasson U, *et al*. Comparison of three Analytical platforms for Quantification of the Neurofilament light chain in blood samples: ELISA, Electrochemiluminescence immunoassay and Simoa. *Clin Chem Lab Med* 2016;54:1655–61.
13 Khalil M, Teunissen CE, Otto M, *et al*. Neurofilaments as biomarkers in neurological disorders. *Nat Rev Neurol* 2018;14:577–89.
14 Kuhle J, Barro C, Disanto G, *et al*. Serum Neurofilament light chain in early Relapsing Remitting MS is increased and correlates with CSF levels and with MRI measures of disease severity. *Mult Scler* 2016;22:1550–9.
15 Modvig S, Degn M, Sander B, *et al*. Cerebrospinal fluid Neurofilament light chain levels predict visual outcome after optic neuritis. *Mult Scler* 2016;22:590–8.
16 Barro C, Benkert P, Disanto G, *et al*. Serum Neurofilament as a Predictor of disease worsening and brain and spinal cord atrophy in multiple sclerosis. *Brain* 2018;141:2382–91.
17 Bittner S, Oh J, Havrdová EK, *et al*. The potential of serum Neurofilament as biomarker for multiple sclerosis. *Brain* 2021;144:2954–63.
18 Kuhle J, Plavina T, Barro C, *et al*. Neurofilament light levels are associated with long-term outcomes in multiple sclerosis. *Mult Scler* 2020;26:1691–9.
19 Lin T-Y, Vitkova V, Asseyer S, *et al*. Increased serum Neurofilament light and thin ganglion cell-inner Plexiform layer are additive risk factors for disease activity in early multiple sclerosis. *Neurol Neuroimmunol Neuroinflamm* 2021;8.
20 Sotirchos ES, Vasileiou ES, Filippatou AG, *et al*. Association of serum Neurofilament light chain with inner retinal layer thinning in multiple sclerosis. *Neurology* 2022;99:e688–97.
21 Costello F. Erythropoietin and optic neuritis in the TONE study. *Lancet Neurol* 2021;20:970–1.
22 Rosenkranz SC, Kaulen B, Zimmermann HG, *et al*. Validation of computer-adaptive contrast sensitivity as a tool to assess visual impairment in multiple sclerosis patients. *Front Neurosci* 2021;15.
23 Tewarie P, Balk L, Costello F, *et al*. The OSCAR-IB consensus criteria for retinal OCT quality assessment. *PLoS One* 2012;7.
24 Motamedi S, Gawlik K, Ayadi N, *et al*. Normative data and minimally detectable change for inner retinal layer thicknesses using a semi-automated OCT image Segmentation pipeline. *Front Neurol* 2019;10.
25 Wasserthal J, Neher P, Maier-Hein KH. Tractseg - fast and accurate white matter tract Segmentation. *Neuroimage* 2018;183:239–53.
26 Sutter R, Hert L, De Marchis GM, *et al*. Serum Neurofilament light chain levels in the intensive care unit: comparison between severely ill patients with and without Coronavirus disease 2019. *Ann Neurol* 2021;89:610–6.
27 Paul F, Calabresi PA, Barkhof F, *et al*. Optical coherence tomography in multiple sclerosis: A 3-year prospective multicenter study. *Ann Clin Transl Neurol* 2021;8:2235–51.
28 Balk LJ, Cruz-Herranz A, Albrecht P, *et al*. Timing of retinal neuronal and axonal loss in MS: a longitudinal OCT study. *J Neurol* 2016;263:1323–31.
29 Balk LJ, Coric D, Knier B, *et al*. Retinal inner nuclear layer volume reflects inflammatory disease activity in multiple sclerosis; a longitudinal OCT study. *Mult Scler J Exp Transl Clin* 2019;5.
30 Gigengack NK, Oertel FC, Motamedi S, *et al*. Structure-function correlates of vision loss in Neuromyelitis Optica spectrum disorders. *Sci Rep* 2022;12:17545.
31 Costello F, Coupland S, Hodge W, *et al*. Quantifying axonal loss after optic neuritis with optical coherence tomography. *Ann Neurol* 2006;59:963–9.
32 Stellmann J-P, Cetin H, Young KL, *et al*. Pattern of gray matter volumes related to retinal thickness and its association with cognitive function in Relapsing-Remitting MS. *Brain Behav* 2017;7.
33 Backner Y, Kuchling J, Massarwa S, *et al*. Anatomical wiring and functional networking changes in the visual system following optic neuritis. *JAMA Neurol* 2018;75:287–95.
34 Balcer LJ, Raynowska J, Nolan R, *et al*. Validity of low-contrast letter acuity as a visual performance outcome measure for multiple sclerosis. *Mult Scler* 2017;23:734–47.
35 Berman S, Backner Y, Krupnik R, *et al*. Conduction delays in the visual pathways of progressive multiple sclerosis patients Covary with brain structure. *Neuroimage* 2020;221.
36 Gabilondo I, Martínez-Lapiscina EH, Martínez-Heras E, *et al*. Trans-Synaptic axonal degeneration in the visual pathway in multiple sclerosis. *Ann Neurol* 2014;75:98–107.
37 Menegaux A, Bäuerlein FJB, Vania A, *et al*. Linking the impact of aging on visual short-term memory capacity with changes in the structural Connectivity of posterior thalamus to occipital Cortices. *Neuroimage* 2020;208.
38 Khalil M, Pirpamer L, Hofer E, *et al*. Serum Neurofilament light levels in normal aging and their association with morphologic brain changes. *Nat Commun* 2020;11:812.
39 Benkert P, Meier S, Schaedelin S, *et al*. Serum Neurofilament light chain for individual prognostication of disease activity in people with multiple sclerosis: a retrospective Modelling and validation study. *Lancet Neurol* 2022;21:246–57.
40 Williams T, Zetterberg H, Chataway J. Neurofilaments in Progressive multiple sclerosis: a systematic review. *J Neurol* 2021;268:3212–22.
41 Leppert D, Kropshofer H, Häring D, *et al*. Author response: blood Neurofilament light in Progressive multiple sclerosis: post hoc analysis of 2 randomized controlled trials. *Neurology* 2022;99:631.
42 Kapoor R, Smith KE, Allegretta M, *et al*. Serum Neurofilament light as a biomarker in Progressive multiple sclerosis. *Neurology* 2020;95:436–44.
43 Barro C, Healy BC, Liu Y, *et al*. Serum GFAP and Nfl levels differentiate subsequent progression and disease activity in patients with progressive multiple sclerosis. *Neurol Neuroimmunol Neuroinflamm* 2023;10.
44 Abdelhak A, Cordano C, Boscardin WJ, *et al*. Plasma Neurofilament light chain levels suggest Neuroaxonal stability following therapeutic Remyelination in people with multiple sclerosis. *J Neurol Neurosurg Psychiatry* 2022.

Visual function resists early neurodegeneration in the visual system in primary progressive multiple sclerosis

SUPPLEMENTAL MATERIAL

SUPPLEMENTAL RESULTS

Associations between outcomes

To illustrate the dependencies on the visual system in total, we examined the association between vision, OCT, sNfL, MRI volumes and other standard MS disability outcomes including cognition, hand function and walking. Spearman correlations and clustering of outcomes are visualized in *Supplementary Figure SF1*. *Supplementary Table ST1* lists the strongest associations based on results from LMER. As expected, outcomes clustered according to their domains, i.e., OCT measures or visual function tests. The strongest association between separate domains was observed between GCIPL and AULCSF (rho = 0·40, LMER: beta = 0·46, $p^{FDR} < 0·001$), followed by the correlation between retinal volume and MD of the POPT (rho = 0·40, LMER beta = -0·42, $p^{FDR} < 0·001$). Cognition measured by the SDMT was associated with optical tract integrity, for example with the MD of the OR (rho = 0·41, LMER beta = -0·28, $p^{FDR} < 0·001$). Absolute sNfL levels showed weak to moderate unadjusted associations with SDMT (rho = 0·33) and RNFL (rho = 0·27) but this was not reproducible in LMER adjusted for age and sex. Other disability scores were not significantly correlated with visual system outcomes.

Supplemental Tables and Figures

Table ST1: Associations between outcomes

Predictor Domain	Predictor variable	Target variable	beta	p^{FDR}
Visual function tests				
	AULCSF[a]	RNFL[b]	0.17	< 0.001
OCT				
	RNFL[b]	AULCSF[a]	0.40	< 0.001
	RNFL[b]	CSFAcuity[c]	0.36	0.002
	retinal volume	POPT[d]	-0.42	0.005
	retinal volume	AULCSF[a]	0.40	< 0.001
	retinal volume	CSFAcuity[c]	0.29	0.007
	retinal volume	HCVA[e]	0.27	0.008
	GCIPL[f]	AULCSF[a]	0.47	< 0.001
	GCIPL[f]	CSFAcuity[c]	0.33	0.001
	GCIPL[f]	HCVA[e]	0.30	0.001
MRI tracts				
	OR[g]	SDMT[h]	-0.28	< 0.001
	POPT[d]	retinal volume	-0.25	0.002
	POPT[d]	EDSS[i]	-0.18	0.002
	SLF_II[j]	GMF[k]	0.20	< 0.001
	SLF_II[j]	BPF[l]	0.17	0.001
MRI volumes				
	GMF[k]	SLF_II[j]	0.37	0.004
Disability				
	EDSS[i]	T25FW[n]	0.34	< 0.001
	EDSS[i]	NHPT[m]	0.28	< 0.001
	SDMT[h]	OR[g]	-0.37	< 0.001
	SDMT[h]	T_OCC[o]	-0.29	0.009
	NHPT[m]	T25FW[n]	0.27	< 0.001
	NHPT[m]	EDSS[i]	0.18	< 0.001
	T25FW[n]	NHPT[m]	0.13	0.001

[a]AULCSF = area under the log contrast sensitivity function; [b]RNFL = retinal nerve fibre layer; [c]CSF Acuity = contrast sensitivity function acuity; [d]POPT = Parieto-occipital pontine; [e]HCVA = high contrast visual acuity; [f]GCIPL = combined ganglion cell and inner plexiform layer; [g]OR = optic radiation; [h]SDMT = Symbol Digit Modality Test; [i]EDSS = expanded disability status scale; [j]SLF_II = superior longitudinal fascicle II; [k]GMF = grey matter fraction; [l]BPF = brain parenchymal fraction; [m]NHPT = 9 hole peg test; [n]T25FW = timed 25-foot walk; [o]T_OCC = Thalamo-occipital. Association between outcomes from different domains based on LMER adjusted for age and sex. Only associations with $p^{FDR} < 0.01$ are shown. None of the models including sNfL levels reached this cut-off.

Figure SF1: Asymmetry between eyes

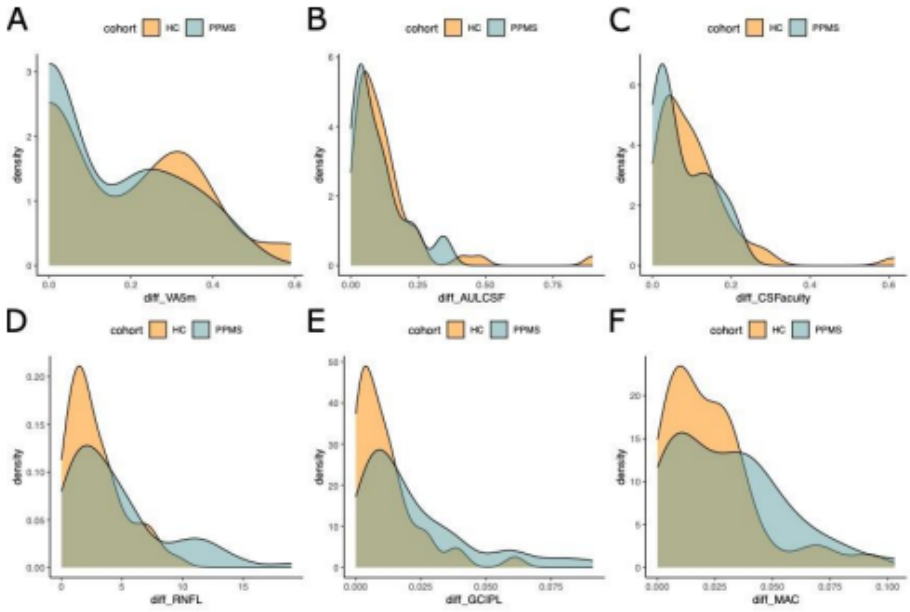

Density plots of inter-eye differences for vision tests and retina. The green area indicates the intersection between the two density plots. (A) High contrast visual acuity, (B) AULCSF, (C) CSF acuity, (D) RNFL thickness, (E) GCIPL volume and (F) retinal volume.

Figure SF2: Associations of outcomes in the visual system

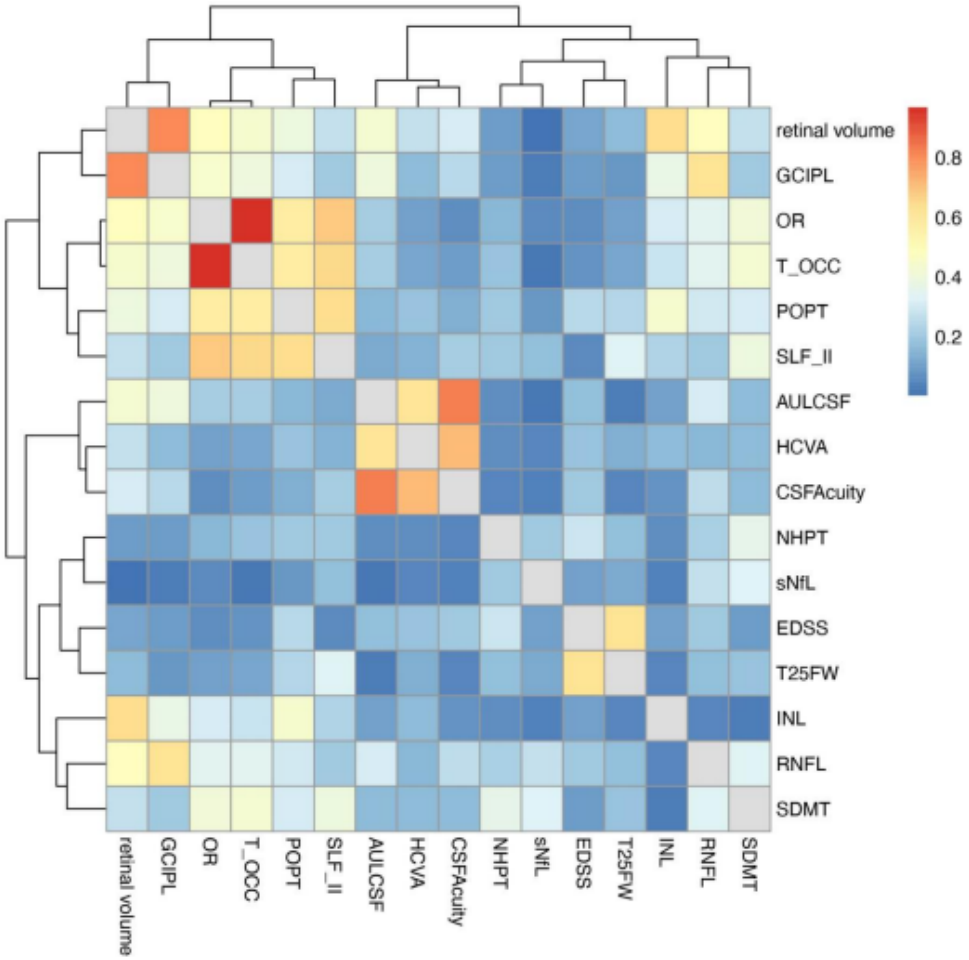

Heatmap of Spearman correlations between visual system metrics, tracts, MRI volumes and clinical scores. Vision: HCVA = High contrast visual acuity, AULCSF = area under the log contrast sensitivity function and CSF Acuity = contrast sensitivity function acuity; OCT: RNFL = peripapillary retinal nerve fiber layer, retinal volume, GCIPL = ganglion cell inner plexiform layer and INL = inner nuclear layer; MRI: OR = optic radiation, POPT = parieto-occipital-pontine tract, SLF_II = superior longitudinal fascicle II (SLF_II), T_OCC thalamo-occipital tract, BPF = brain parenchymal fraction, GMF = grey matter fraction; sNfL = absolute serum neurofilament light chain; Clinical scores: EDSS = expanded disability status scale (overall disability), SDMT = Symbol Digit Modality Test (cognition), T25FW = timed 25 foot walk (mobility), NHPT = 9 hole peg test (manual dexterity).

SF3: Scatterplots for all significant spearman correlations in figure SF2

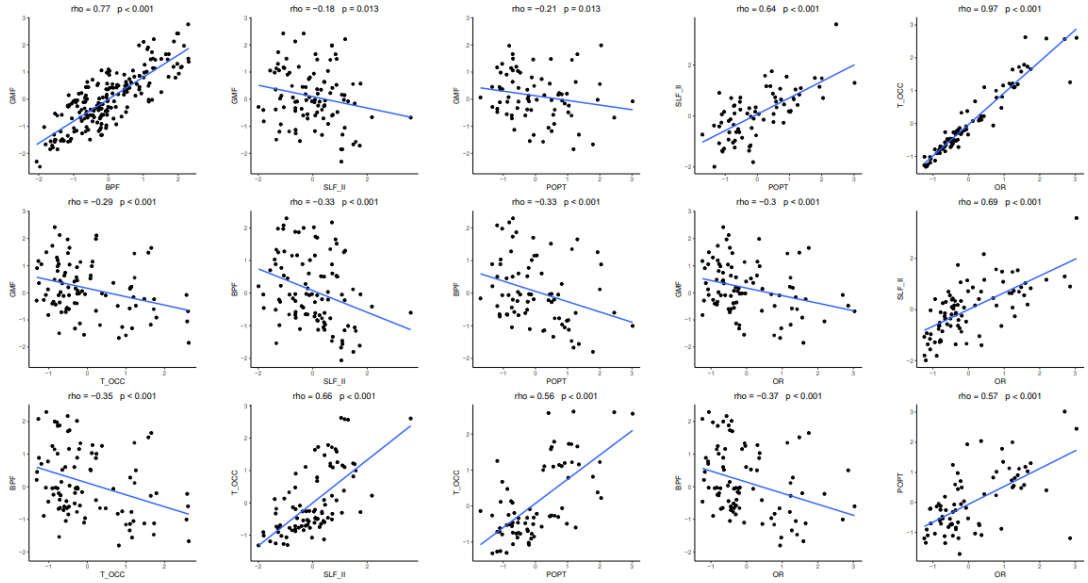

Data scaled, blue line is the regression estimate from a simple linear regression. Confidence interval in grey.

SF3: Scatterplots for all significant spearman correlations in figure SF2

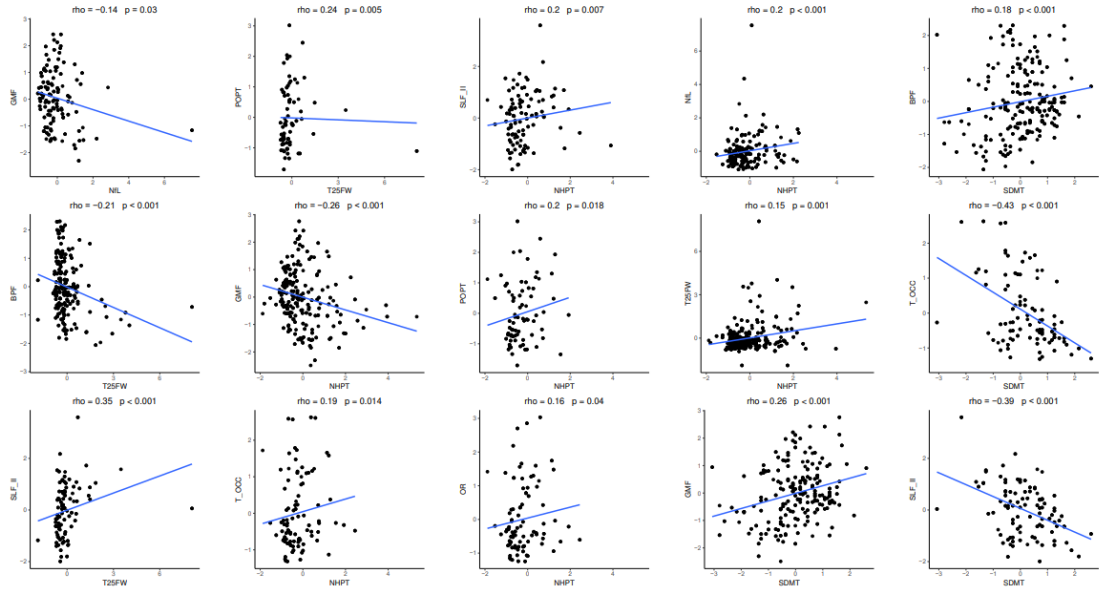

Data scaled, blue line is the regression estimate from a simple linear regression. Confidence interval in grey.

SF3: Scatterplots for all significant spearman correlations in figure SF2

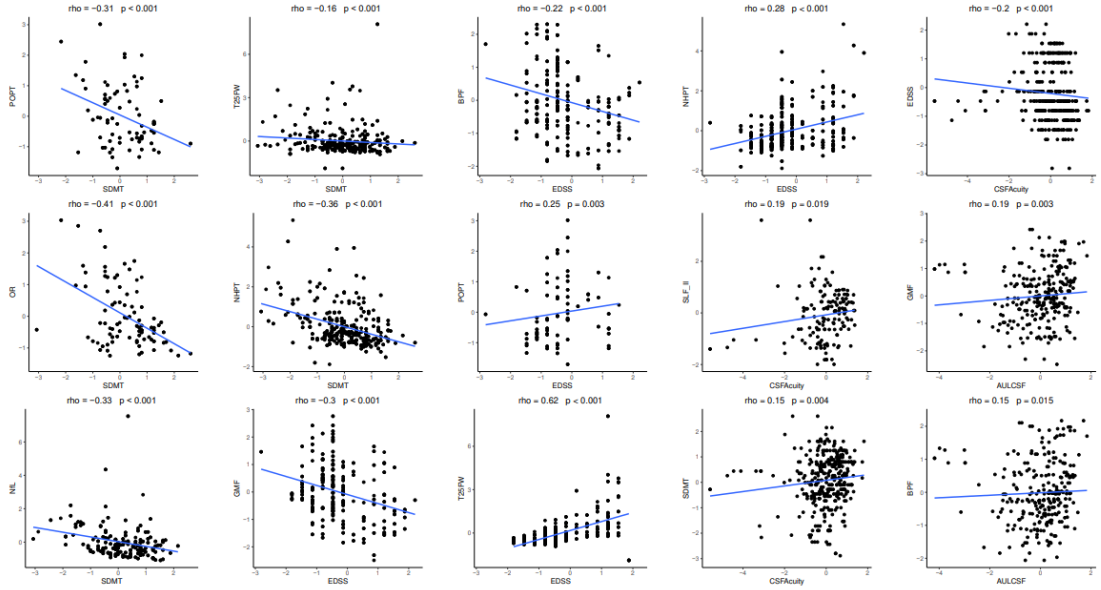

Data scaled, blue line is the regression estimate from a simple linear regression. Confidence interval in grey.

SF3: Scatterplots for all significant spearman correlations in figure SF2

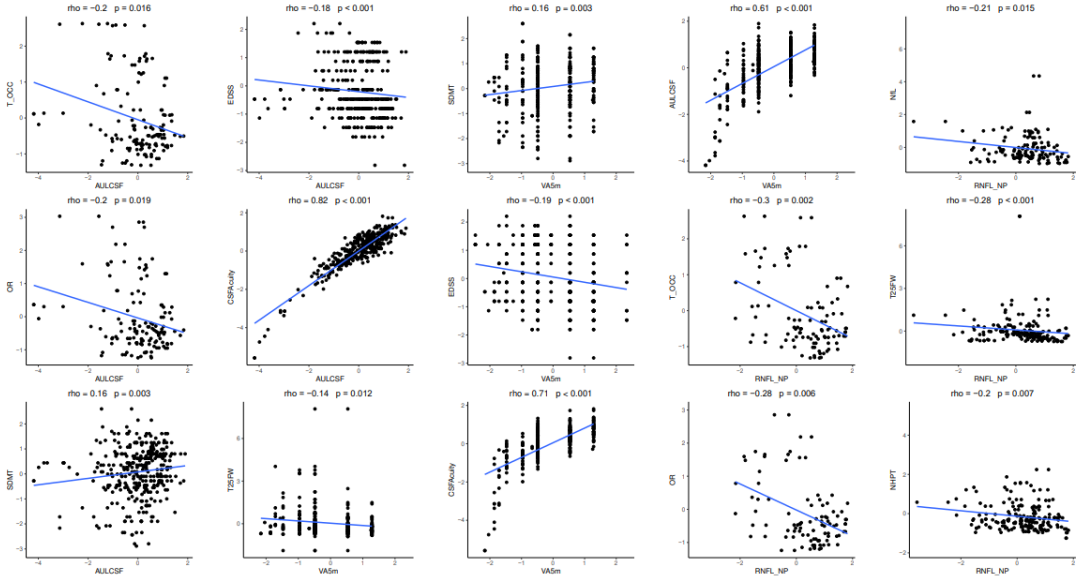

Data scaled, blue line is the regression estimate from a simple linear regression. Confidence interval in grey.

SF3: Scatterplots for all significant spearman correlations in figure SF2

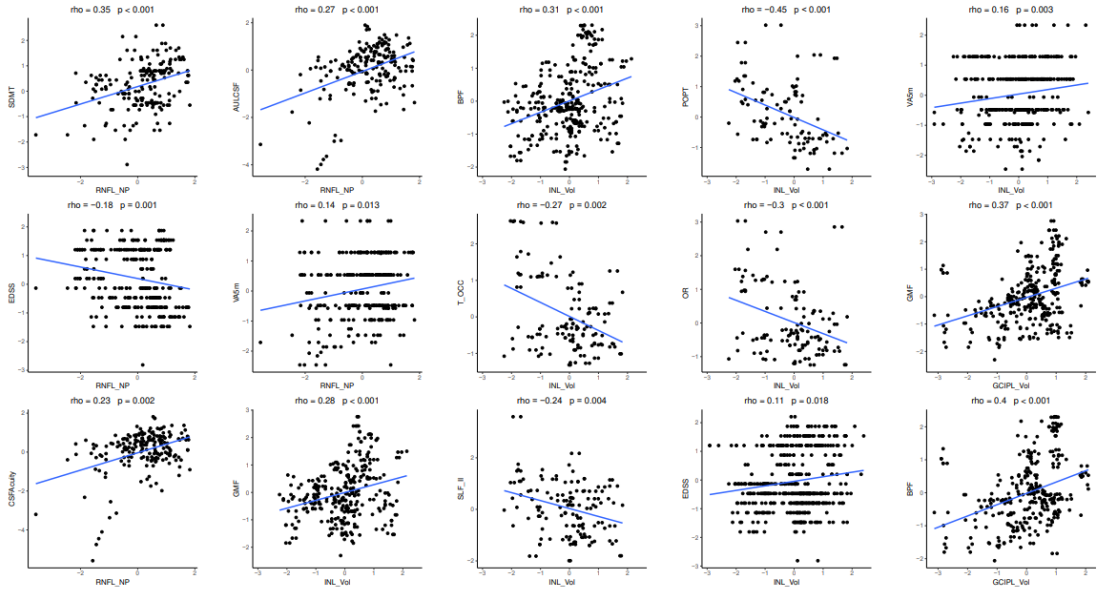

Data scaled, blue line is the regression estimate from a simple linear regression. Confidence interval in grey.

SF3: Scatterplots for all significant spearman correlations in figure SF2

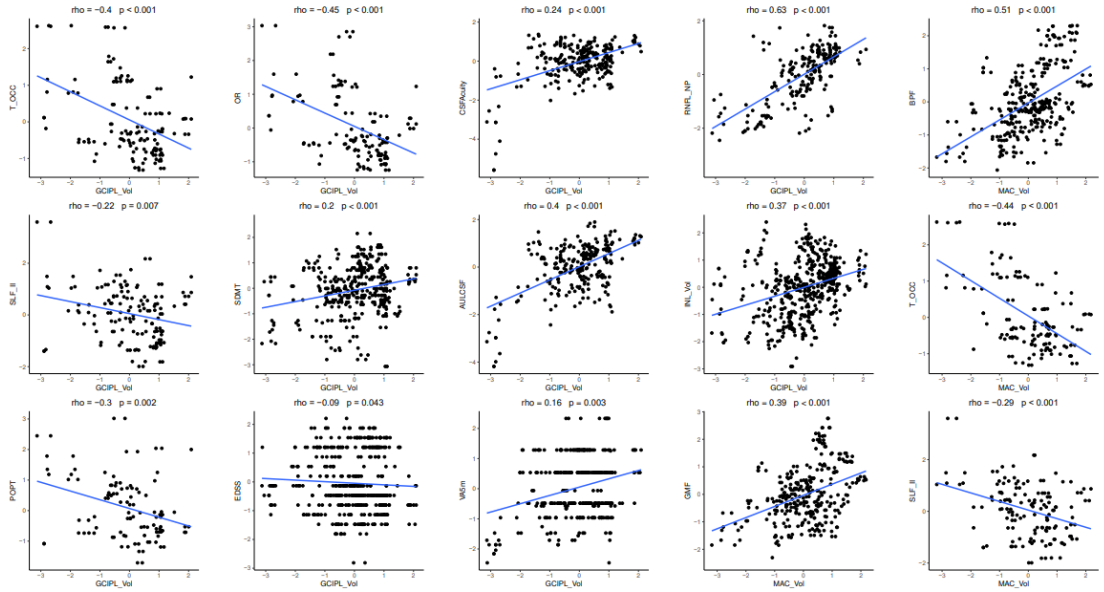

Data scaled, blue line is the regression estimate from a simple linear regression. Confidence interval in grey.

SF3: Scatterplots for all significant spearman correlations in figure SF2

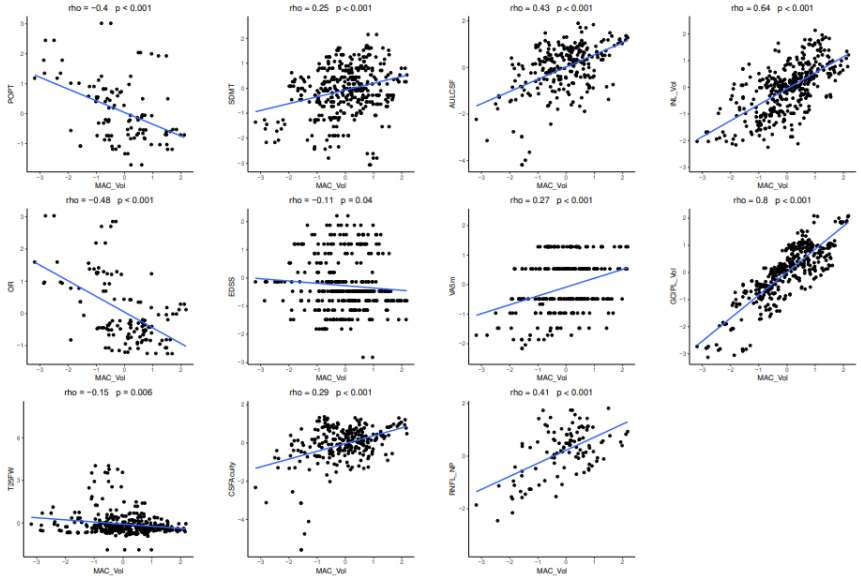

Data scaled, blue line is the regression estimate from a simple linear regression. Confidence interval in grey.

Diversity statement – detailed citation report

Figures as produced with the cleanBib tool: https://github.com/dalejn/cleanBib

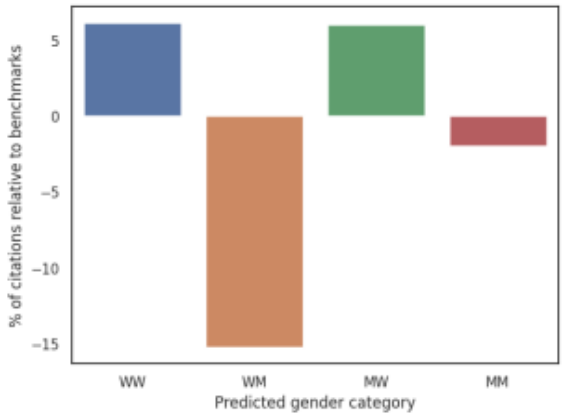

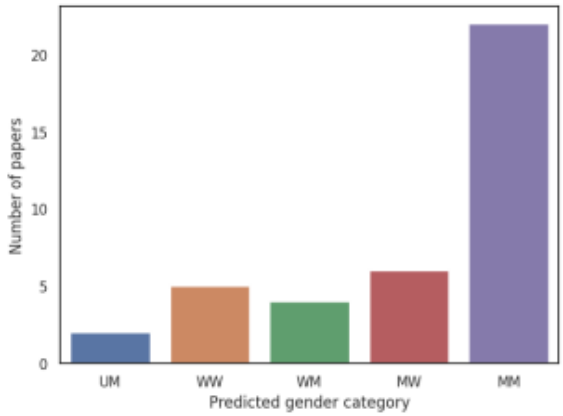

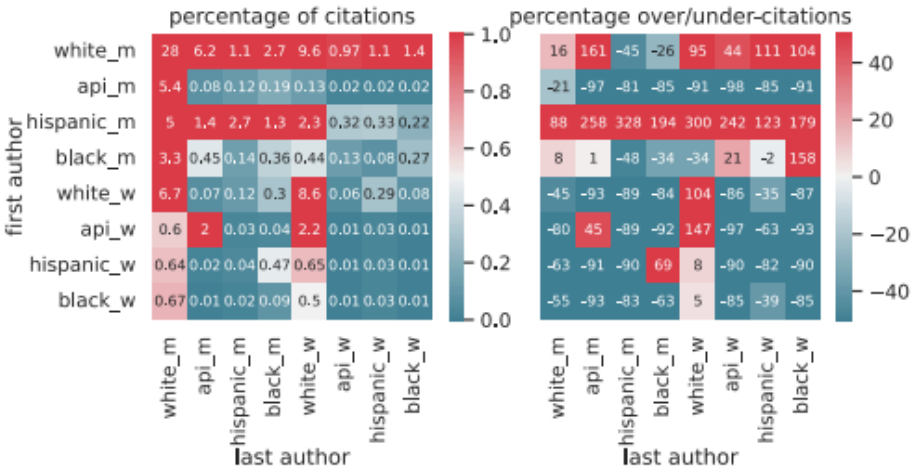

Nine-Point Advised Protocol for OCT Study Terminology and Elements (APOSTEL) 2.0 Checklist

Item Category		Manuscript
1 Study protocol	(1) Describe how many OCT operating sites and graders were included (2) Report the timing of OCT compared to other measurements (same day, delayed) (3) Describe the inclusion and exclusion criteria (4) In case of limited word count, consider submitting the exact methodology as supplementary material[a]	3. Material and methods : 3.1 Participants and 3.3 OCT protocol and processing
2 Acquisition device	For all OCT devices used, report data on: (1) Manufacturer (2) Model (3) Version (4) Software version (5) Device type (time/spectral domain, swept-source, adaptive optics)[a]	3. Material and methods : 3.3 OCT protocol and processing
3 Acquisition settings	Clearly describe the settings in which OCT scans were obtained: (1) Pupils dilated before examination (y/n) (2) Number of operators and devices[b]	3. Material and methods : 3.3 OCT protocol and processing
4 Scanning protocol	Clearly describe the scanning protocol, including: (1) Type of scan (circular, volume, star, line, other) (2) Location (area of interest, macula, optic nerve head, papillomacular bundle, other) (3) Scan parameters (with or without eye tracking) Volume scan: size of scan, area and location of measurement (degrees or millimeters), number of B-scans, alignment of B-scans, number of A-scans per B-scan[a] Radial scan: size of scan area (degrees or millimeters), number of B-scans, alignment of B-scans, number of A-scans per B-scan Ring scan: diameter, A-scans/B-scan, manual or automatic placement of ring or method of centering, depth resolution Line scan: angle, location, number of A-scans, depth resolution	3. Material and methods : 3.3 OCT protocol and processing
5 Funduscopic imaging	Report other imaging modalities used in addition to OCT (funduscopy, confocal scanning laser ophthalmoscope, retinal angiography, autofluorescence imaging, etc.) (2) Describe acquisition protocol, including: Excitation wavelength Filter sets Number of frames averaged (if applicable) Report device specific features when utilized (e.g., enhanced depth imaging, swept-source OCT, adaptive optics)[a]	NA
6 Postacquisition data selection	Describe image selection process, including: (1) Quality control criteria (2) Postacquisition discard (number and criteria) (3) Eye selection strategy (if applicable)	3. Material and methods : 3.3 OCT protocol and processing
7 Postacquisition analysis	Describe all postacquisition steps: (1) Software used for processing scans and segmentation (may be different from acquisition software) (2) Which individual retinal layers were segmented/included (3) Method of segmentation (automated, semi-automated, or manual) (4) How potential bias was addressed in the case of manual segmentation or manual correction of automated segmentation errors (masking)[a] (5) Grid used for data extraction (size, shape, selected sections) (6) Pixel to millimeter ratio if images are exported (caliper need)[a]	3. Material and methods : 3.3 OCT protocol and processing
8 Nomenclature and abbreviations	Define: (1) Anatomical structures analyzed (2) Units of provided measurements (e.g., volume or thickness) (3) Report the number of eyes presenting additional retinal pathology; describe qualitative retinal changes and report exact methodology of quantification[a]	3. Material and methods : 3.3 OCT protocol and processing

9 Statistical approach	Statistical models used for the analyses of OCT data (2) Whether data were analyzed by eye or by patient	3. Material and methods : 3.6 Statistical analysis

2. Darstellung der Publikation mit Literaturverzeichnis

2.1 Einleitung

Die Multiple Sklerose (MS) ist eine chronisch-entzündliche Erkrankung, bei der es schubweise oder, wie bei der primär progredienten Verlaufsform (PPMS), kontinuierlich zu einer zunehmenden Neurodegeneration und infolgedessen zu einer zunehmenden Behinderung kommt.[1] Um Neurodegeneration frühzeitig feststellen zu können, bedarf es Biomarker, die als Prädiktoren für den klinischen Verlauf dienen können.

Dafür kommt die Atrophie von retinalen Nervenschichten, wie der retinalen Nervenfaserschicht (RNFL), der Ganglienzellschicht und inneren plexiformen Schicht (GCIPL) sowie der inneren Körnerschicht (INL) infrage. Diese kann präzise mithilfe der Optischen Kohärenztomografie (OCT) bestimmt werden.[2,3] Eine Reduktion der RNFL und GCIPL wurde in MS Patienten bereits beobachtet und war mit dem Hochkontrast- und Niedrigkontrastsehen, kortikaler Atrophie und kognitiver Beeinträchtigung assoziiert.[2,4–6] Die meisten Studien dazu beziehen sich auf Patienten mit schubförmig remittierender Multipler Sklerose (RRMS). Nur in wenigen wurden PPMS Patienten, meist mit einer niedrigen Fallzahl, eingeschlossen.[7,8]

Ein anderer möglicher Neurodegenerationsmarker ist das Protein Neurofilament Light Chain im Serum (sNfL). Dieses ist ein Bestandteil des axonalen Cytoskeletts und wird bei axonaler Schädigung in den Liquor und in geringerer Konzentration in das Serum freigesetzt.[9] Zahlreiche Studien stellten einen Zusammenhang zwischen der sNfL Konzentration und Indikatoren der Krankheitsaktivität von MS Patienten, wie der Aktivität im MRT, Hirnatrophie, Retrobulbärneuritis und der Schubrate dar.[10,11] Jedoch ist noch nicht vollständig geklärt, ob sich mit dem sNfL die langfristige Krankheitsprogression, vor allem bei Patienten mit PPMS, vorhersagen lässt.[12,13]

Unsere Hypothese ist, dass Biomarker des visuellen Systems als Prädiktoren des Krankheitsverlaufs in PPMS Patienten dienen können und präziser sind als die aktuell verwendeten prädiktiven Biomarker, wie die sNfL. Wir stellen eine große Beobachtungsstudie mit PPMS Patienten vor, welche longitudinale Sehleistungs-, OCT-, MRT- und sNfL-Messungen sowie einen querschnittlichen Vergleich mit gesunden Probanden beinhaltet.

2.2 Methoden

Patienten mit PPMS wurden im Zeitraum von 2012 bis 2018 in der MS Tagesklinik des Universitätsklinikums Hamburg-Eppendorf (UKE) und dem NeuroCure Clinical Research Center der Charité, Universitätsklinikum Berlin rekrutiert. Die Einschlusskriterien waren die Diagnose PPMS nach den McDonald Kriterien 2010, ein Expanded Status Disability Scale (EDSS) von maximal 7,0 und ein Alter von 18 bis 65 Jahren. Patienten mit erheblichen gesundheitlichen Einschränkungen neben der MS sowie Kontraindikationen für ein MRT wurden von der Studie ausgeschlossen. Alterskorrelierte gesunde Kontrollen wurden am UKE rekrutiert.

Die Patienten wurden jährlich untersucht, der EDSS erhoben, der Timed-25-Foot-Walk-Test (T25FWT), Symbol-Digit-Modalities-Test (SDMT) und der Nine-Hole-Peg-Test (NHPT) wurden durchgeführt. Für jedes Auge wurden separat der Hochkontrast-Fernvisus (high contrast visual

acuity, HCVA) und die Funktion aus der Kontrastemfindlichkeit und der Ortsfrequenz (conrast sensitivity function, CSF) bestimmt. Aus der CSF errechneten wir die Fläche unter der logarithmierten CSF (area under the log CSF, AULCSF), die Ortsfrequenz, welche bei vollem Kontrast gerade noch erkannt wird (CSF Acuity)[14] sowie die Kontrastsensitivität für bestimmte Ortsfrequenzen (1,5; 3; 6; 12 und 18 Perioden/Grad). Blutproben wurden entnommen und an das Universitätsklinikum Basel, Schweiz verschickt, wo das Protein Neurofilament Light Chain im Serum (sNfL) bestimmen wurde.

Mithilfe der Optischen Kohärenztomographie wurden die Dicke der peripapillären retinalen Nervenfaserschicht (retinal nerve fiber layer, RNFL), die Volumina der makulären Retina, der makulären Ganglienzellschicht und inneren plexiformen Schicht (ganglion cell/inner plexiform layer, GCIPL) sowie der makulären inneren Körnerschicht (inner nuclear layer, INL) bestimmt. Dafür verwendeten wir das Spectralis SD-OCT (Heidelberg Ingeneering). Für die Messung der pRNFL wurden ein Ringscan von 12° um die Papille und für die makulären Schichten ein Boxscan der Makula von 25°x30° Grad aufgenommen. Die Nervenfaserschichten wurden semiautomatisch segmentiert. Aufnahmen, die nicht den OSCAR-IB Kriterien[15] entsprachen, wurden ausgeschlossen. Eine Differenz der RNFL-Dicke von über 6µm zwischen den Augen eines Probanden wurde als Hinweis für eine subklinische Optikusneuritis (sON) angesehen.

Wir fertigten T1 und T2 gewichtete MRT Aufnahmen mit dem Skyra 3T an und berechneten die Volumina der grauen und weißen Substanz sowie des Gesamthirnvolumens. Von 42 Patienten wurden mithilfe der Diffusions-Tensor-Bildgebung auch die mittleren Diffusionswerte von vier Bündeln der weißen Substanz bestimmt: der optischen Strahlung (optic radiation, OR), des Parieto-Okzipital-Pontinen Bündels (parieto-occipital-pontine tract, POPT), des Superioren Longitudinalen Faszikels II (superior longitudinal fascicle II, SLF_II) und des Thalamo-Okzipitalen Bündels (thalamo-occipital tract, T_OCC). Ein erhöhter Diffusionswert ist mit Pathologien von Nervengewebe assoziiert und wurde bei verschiedenen neuropsychiatrischen Erkrankungen sowie als Folge des Alterungsprozesses nachgewiesen[16].

Die statistische Auswertung erfolgte mit R V.4.2.1. Die deskriptive Statistik ist mit Mittelwerten und Standardabweichungen oder mit Medianen und Spannweiten oder Häufigkeiten dargestellt. Gruppen wurden mit den Mixed Models verglichen. Hierbei wird berechnet, in wieweit eine abhängige Variable von einem uns interessierenden Faktor (Fixed Factor) und uns nicht interessierenden, aber wahrscheinlich relevanten Faktoren (Random Factors) beeinflusst wird [17]. Als Random Factors definierten wir das Alter, das Geschlecht sowie den Hinweis auf eine subklinische optische Neuritis (intraindividueller RNFL- Dickenunterschied von >6µm). Für die durchschnittlichen Parameter in der Patientengruppe wurden Perzentilen bezogen auf die Kontrollgruppe ermittelt. Um Wendepunkte der Funktion von Sehleistungsparametern und strukturellen Komponenten des visuellen Systems zu bestimmen, wurde die für Alter, Geschlecht und sON korrigierte segmentierte Regression angewendet. Schließlich wurden die Patienten in eine Gruppe mit AULCSF Verlust und ohne AULCSF Verlust im follow-up unterteilt. Mithilfe der Varianzanalyse (ANOVA) korrigiert für Alter, Geschlecht und sON wurde die Assoziation von Gruppenzugehörigkeit und der Veränderung der gemessenen klinischen Parameter über die Zeit analysiert. Ein p-Wert von <0.05 wurde als statistisch signifikant angesehen.

2.3 Ergebnisse

81 Patienten mit PPMS und zwei Kontrollkohorten mit jeweils 52 Probanden wurden in die Studie eingeschlossen. Die Patienten litten durchschnittlich unter einem moderaten Krankheitsstadium mit einem EDSS von 3,5 (2.0.-7.0) und einer durchschnittlichen Krankheitsdauer von 5,9 Jahren (36,0-69,0; SD: 7,7). Die durchschnittliche Follow-up Zeit betrug 2,7 Jahre (SD 1,7; bis zu 6 Jahren). Nur insgesamt vier Patienten erhielten am Anfang der Studie immunmodulatorische Medikamente, im Verlauf der Studie kamen fünf weitere Patienten dazu. Die Patientengruppe unterschied sich in der Geschlechtsverteilung und der Altersverteilung signifikant von jeweils einer der Kontrollgruppen, weshalb folgende Analysen neben der sON für Alter und Geschlecht korrigiert wurden.

Eine peripapilläre RNFL-Dickendifferenz von 5-6µm zwischen den Augen eines Individuums wurde von Nolan et al. 2022 als sinnvoller Grenzwert zur Identifikation der optischen Neuritis vorgeschlagen.[18] 15 von 79 unserer Patienten (19%; 95% CI 11% bis 29%) und 5 von 44 Kontrollen (11%; 95% CI 4%-26%) mit Messungen beider Augen wiesen eine intraindividuelle RNFL-Dickendifferenz von > 6µm am Beginn der Studie auf. Patienten und Kontrollen unterschieden sich diesbezüglich nicht signifikant (p=0.39).

Wir untersuchten, ob in der Patientengruppe insgesamt mehr intraindividuelle Unterschiede von Sehleistungsparametern und strukturellen Komponenten des visuellen Systems vorliegen als in der Kontrollgruppe. Häufigkeitsplots dazu zeigen, dass sich die Kurven für intraindividuelle Unterschiede bezüglich der VA5m, AULCSF und CSF Acuity von Patienten und Kontrollen weitestgehend decken. Bezüglich der RNFL Dicke und des GCIPL- und totalen Makulavolumens zeigen die Kurven der Kontrollgruppe jedoch höhere Peaks für geringe intraindividuelle Unterschiede als die Kurven der Patientengruppe. Die Kurve der Gesunden flacht ab einer intraindividuellen RNFL-Dickendifferenz von über 10 µm fast auf eine Häufigkeit von 0 ab, die dazugehörige Kurve der Patienten jedoch nicht. Deshalb kann eine intraindividuelle RNFL-Dickendifferenz von über 10 µm als mögliches zukünftiges diagnostisches Kriterium für das Vorliegen einer PPMS oder Retrobulbärneuritis diskutiert werden.

Zunächst erfolgte ein querschnittlicher Vergleich klinischer Parameter zwischen der Patienten- und Kontrollgruppe am Anfangspunkt der Studie. Wir beobachteten bei den PPMS Patienten eine verminderte AULCSF, CSF Acuity und Kontrastsensitivität für höhere Ortfrequenzen, wohingegen die HVCA keinen signifikanten Unterschied zeigte. Passend dazu waren auch die RNFL Dicke und das GCIPL Volumen in Patienten verringert. Interessanterweise gab es unabhängig von Alter, Geschlecht und sON keine signifikanten Unterschiede der Hirnvolumina und der mittleren Diffusionskoeffizienten. Die sNfL Werte waren in der Patientengruppe erhöht.

Als Nächstes untersuchten wir, inwiefern die Parameter von der Krankheitsdauer am Anfangspunkt der Studie abhingen. Dabei zeigte die Krankheitsdauer mit keinem Parameter der Sehleistung (AULCSF, CSF Acuity, HCVA) eine signifikante Assoziation. Jedoch nahmen die RNFL Dicke um 0,55 µm/Jahr (95% KI 0,13 bis 0,96; p = 0.010), das Makulavolumen um 0,006 $\mathrm{mm}^3/\mathrm{Jahr}$ (95% KI 0,002 bis 0,010, p= 0,007) und das GCIPL Volumen um 0.004 $\mathrm{mm}^3/\mathrm{Jahr}$ (95% KI 0,0001 bis 0,007$\mathrm{mm}^3/\mathrm{Jahr}$, p= 0,002) mit zunehmender Krankheitsdauer ab. Das INL Volumen zeigte keine signifikante Änderung. Der mittlere Diffusionskoeffizient stieg nur für den T_OCC um 0,06x $10^{-3}\,\mathrm{mm}^2/\mathrm{s}$ pro Krankheitsjahr an, die mittleren Diffusionskoeffizienten für andere Bündel veränderten sich nicht signifikant. Auch die absoluten sNfL Werte korrelierten nicht mit der Krankheitsdauer (beta=-0.15, 95% KI -0,42 bis

0.11, p=0,050, z-Scores nahmen aber um 0,04/Krankheitsjahr (95% KI 0 bis 0,08, p=0,050) ab. Wir berechneten die Perzentilen der durchschnittlichen Werte der Sehtestparameter, retinalen Schichten und des sNfL in Abhängigkeit von der Krankheitsdauer. Zum Zeitpunkt der Diagnosestellung (Krankheitsdauer = 0) lagen die INL und das sNfL im oberen Perzentilenbereich, die HCVA, AULCSF sowie das retinale Makulavolumen in der Nähe der 50. Perzentile, die CSF Acuity, RNFL und GCIPL waren erniedrigt.

Uns interessierte nun, inwiefern die Neurodegeneration der retinalen Schichten und der neuronalen Bündel die Sehfähigkeit beeinflussen. Es zeigte sich, dass die Parameter der Sehleistung (HCVA, AULCSF, CSF Acuity) mit fortschreitender Abnahme der GCIPL- und RNFL-Dicke lange weitestgehend stabil blieben. Dies war bis zu einem Wendepunkt der Fall (RNFL = 90,6 µm; 95% KI 84,9 bis 96,3; p = <0.001 und GCIPL = 0,43 μm^3 ; 95% KI 0,40 bis 0,46; p = <0.001), nach dem die drei Parameter deutlich zu sinken begannen. Dabei zeigte die AULCSF einen steileren Abstieg als die anderen Sehleistungsparameter. SLF_II zeigte ab einem mittleren Diffusionskoeffizienten von 0,76 10x $10^{-3}\ mm^2/s$ (95% KI 0,74 bis 0,78; p<0.001) einen steileren AULCSF Abstieg. Nur ein sehr hoher mittlerer Diffusionswert für T_OCC konnte als Wendepunkt bestimmt werden, alle anderen neuronalen Bündel und das sNfL zeigten keinen Wendepunkt.

Da die AULCSF ein sensitiverer Parameter zur Bestimmung der Sehleistung zu sein scheint als die HCVA und CSF Acuity, unterteilten wir die Patienten in eine Gruppe mit einem AULCSF Abstieg (AULCSF Betakoeffizient <0; n= 25) und eine Gruppe ohne Abstieg (n=26). Die Gruppe mit einem AULCSF Abstieg zeigte auch einen Abstieg der HCVA (beta= -0,09/Jahr, p=0,005), CSF Acuity (beta=-0,03/Jahr, p=0,007) sowie einen schnelleren EDSS Anstieg (beta= 0,17/Jahr, p=0,043). Interessanterweise nahm die GCIPL Dicke in der AULCSF Abstiegsgruppe weniger ab als in der Gruppe der Patienten mit stabiler AULCSF (beta=0,004 mm^3/Jahr, p=0,028). Bezüglich der Entwicklung der RNFL Dicke, der INL Dicke, des retinalen Makulavolumens, des NHPT, T25WT, SDMT und der sNfL unterschieden sich die beiden Gruppen nicht.

2.4 Diskussion

Unsere querschnittliche Analyse zeigte, dass PPMS Patienten eine signifikant geringere RNFL Dicke, ein geringeres GCIPL Volumen und einen Trend zum geringeren retinalen Makulavolumen verglichen mit gesunden Probanden aufweisen. Dies steht im Einklang mit den Ergebnissen einer anderen PPMS Patienten einschließenden Studie. [4] Die Abnahme der RNFL Dicke pro Krankheitsjahr unserer PPMS Kohorte ist vergleichbar mit der von RRMS Patienten ohne Zustand nach Retrobulbärneuritis.[19,20] Zudem konnten wir zeigen, dass der Zusammenhang zwischen retinalem Substanzschaden und der Sehleistung nicht linear ist, sondern ein Wendepunkt existiert, ab dem es zu einer beschleunigten Verschlechterung der Sehleistung kommt. Dieser lag in unserer PPMS Kohorte bei einer pRNFL-Dicke von 92.1 µm bezogen auf die AULCSF. Er ist somit wesentlich höher als der bestimmte Wendepunkt bei Patienten mit MS oder anderen neurodegenerativen Erkrankungen, wenn die Sehleistung mit Standardsehtafeln bestimmt wird.[21,22]

Eine intraindividuelle pRNFL Differenz von mindestens 6µm, welche zuvor als Kriterium für einen Hinweis für eine Retrobulbärneuritis vorgeschlagen wurde, erscheint nicht spezifisch genug. Laut unseren Ergebnissen erscheint ein Cuf-off- Wert von 10µm sinnvoll, diesbezüglich sind jedoch weitere Analysen nötig. Das 6µm Differenz Kriterium korrelierte mit Parametern

der CSF, jedoch nicht relevant mit anderen klinischen Outcomes. Die asymmetrische retinale Atrophie in PPMS Patienten könnte auch auf eine nicht balancierte Hirnatrophie und weniger auf eine subklinische Retrobulbärneuritis zurückzuführen sein.[23]

Wir konnten eine Korrelation zwischen der Atrophie von pRNFL, GCIPL und dem retinalen Volumen und Sehleistungsparametern, nicht aber von INL und klinischen Outcomes feststellen. Mithilfe der CSF ließ sich die abnehmende Sehleistung früher detektieren als mit den Standard-Hochkontrastsehtafeln. Von einer höheren Sensitivität und besseren Korrelation mit klinischen Outcomes des Niedrigkontrastsehens wurde bereits berichtet.[24] Zudem korrelierte die Atrophie von retinalen Nervenschichten mit Diffusionskoeffizienten von neuronalen Bündeln im Gehirn, was ein weiterer Hinweis für trans-synaptische Degeneration in PPMS Patienten ist.[25]

Wir beobachteten in Patienten mit einer stabilen AULCSF im Krankheitsverlauf eine stärkere Reduktion des GCIPL Volumens als bei Patienten mit AULCSF Abnahme. Jedoch zeigte sich bei Patienten mit einer AULCSF Progression eine schnellere Zunahme des EDSS. Dies zeigt die Komplexität der Krankheitsentwicklung in PPMS Patienten und die Notwendigkeit einer genauen individuellen Evaluation des Krankheitsstatus. Eine Rolle hierin kann die Robustheit des visuellen Systems gegen strukturellen Schaden spielen.

Das sNfL war im querschnittlichen Vergleich zwar in der Patientengruppe erhöht, die absoluten sNfL Werte korrelierten jedoch nicht mit der Krankheitsdauer. Da die sNfL Konzentration mit dem Alter steigt[26], berechneten wir die z-Scores, welche die Abweichung von einer Kontrollkohorte widerspiegeln.[27] Diese zeigten einen Trend zur Abnahme mit zunehmender Krankheitsdauer. Eine starke Korrelation von sNfL und der retinalen Atropie oder anderen klinischen Parametern konnten wir nicht feststellen. Größere longitudinale Datensätze könnten möglicherweise Confounder, wie den Body Mass Index, Läsionen und Atrophie des Zentralen Nervensystems identifizieren und komplexere Zusammenhänge zwischen dem sNfL und Kranheitsmerkmalen aufdecken. Andere Studien mit MS Patienten zeigten eine Korrelation von sNfL und der Entzündungsaktivität sowie klinischen Outcomes.[11,28] Mithilfe der sNfL Konzentration im Liquor zu Beginn der Optikusneuritis konnten die Niedrigkontrastsehkraft, RNFL und GCIPL im Verlauf vorhergesagt werden.[29]

Unsere Studie hat mehrere Limitationen, wie fehlende Messungen visuell evozierter Potentiale, funktionaler MRTs und in der Gruppe der gesunden Kontrollen das Fehlen einer Diffusionsbildgebung sowie longitudinaler Daten. Denkbar ist auch ein Bias durch die Datenerhebung in zwei verschiedenen Zentren und zwei Kontrollkohorten für sNfL und das visuelle System. Trotz der Größe unserer Kohorte und der vergleichsweise langen Follow-up Zeit lassen sich nur eingeschränkt Aussagen über eine Krankheit machen, die sich über Jahrzehnte entwickelt.

2.5 Einordnung in den breiteren Kontext

Unsere Studie zeigte, dass zwischen der Atrophie der retinalen Nervenschichten und der Sehleistung kein linearer Zusammenhang besteht, sondern die Sehleistung erst ab einem bestimmten kritischen Wert des Gewebeschwunds merklich zu sinken beginnt. Dieser lag bei 90,6 µm für die peripapilläre RNFL und bei 0,43 μm^3 für die makuläre GCIPL. Zu ähnlichen Ergebnissen kamen Gigengack et al. in ihrer Studie zu Patienten mit den Neuromyelitis-optica-Spektrum-Erkrankungen (NMOSD), MOG-Antikörper assoziierten Erkrankungen (MOGAD) und RRMS. Hier wurde für eine Dicke von über 60µm pRNFL oder GCIPL keine oder nur eine

sehr geringe Assoziation von retinaler Nervensubstanz und der Sehleistung gefunden. Ab einem Wert von unter 60µm war eine zunehmende Atrophie von pRNFL und GCIPL mit einer Reduktion des Hochkontrast- und Niedrigkontrastsehens sowie mit zunehmenden Gesichtsfeldausfällen in allen Krankheitsgruppen assoziiert.[21] Dies zeigt, dass eine Robustheit des visuellen Systems bis zu einer bestimmten Ausprägung der Netzhautatrophie nicht nur bei Patienten mit MS, sondern auch bei anderen neurodegenerativen Erkrankungen besteht. Beim Offenwinkelglaukom werden Gesichtsfeldausfälle erst detektierbar, wenn die Nervensubstanz der Papille bereits auf unter ein Drittel des normalen Wertes ausgedünnt ist.[30] Erst ab einem Verlust von 17,3% der RNFL wurden in Glaukompatienten anfängliche Gesichtsfelddefekte beobachtet.[31] Eine andere Studie zeigte, dass die mittlere RNFL Dicke, die mit anfänglichen Gesichtsfelddefekten in Gaukompatienten assoziiert ist, 89 µm beträgt.[32] Eine Erklärung für die Robustheit des visuellen Systems könnte die Neuroplastizität auf Ebene des zentralen Nervensystems sein. Bei pädiatrischen MOGAD Patienten erholte sich die Sehleistung nach einer Optikusneuritis bei ähnlicher Atrophie der RNFL, GCIL, INL und des totalen Makulavolumens wesentlich besser als bei adulten MOGAD Patienten. Die altersabhängige Neuroplastizität des visuellen Systems auf kortikaler Ebene wurde hierfür als mögliche Ursache vorgeschlagen.[33] Auch kompensatorische Mechanismen auf retinaler Ebene sind denkbar, hier sind weitere Analysen sinnvoll.

Unsere Ergebnisse identifizierten die AULCSF als sensitiveren Parameter als die HCVA oder die CSF Acuity. Die AULCF wies einen steileren Abstieg mit zunehmender RNFL und GCIPL Atrophie auf als die beiden anderen Sehleistungsparameter. Auch im querschnittlichen Vergleich mit gesunden Probanden waren die AULCSF, CSF Acuity und die Kontrastsensitivität für höhere Ortfrequenzen bei PPMS Patienten vermindert, wohingegen die HVCA sich nicht signifikant unterschied. Eine höhere Sensitivität des Niedrigkontrastsehens sowie eine bessere Korrelation mit klinischen Outcomes wurde nicht nur bei MS Patienten[24], sondern auch bei einer Vielzahl von neurodegenerativen und ophthalmologischen Erkrankungen beobachtet. Die meisten Studien, welche Patienten mit Morbus Alzheimer einschlossen, konnten kein vermindertes Hochkontrastsehen verglichen mit Gesunden feststellen. Jedoch fanden mehrere Studien ein vermindertes Kontrastempfinden bei Alzheimer Patienten.[34] Verglichen mit dem Hochkontrastsehen korrelierte die Kontrastsensitivität besser mit der subjektiv erlebten Seheinschränkung in Katarakt Patienten[35] sowie mit der sehleistungsbezogenen Lebensqualität in Patienten mit altersbedingter Makuladegeneration.[36] Die computergestützte Bestimmung der Kontrastsensitivitätsfunktion (qCSF), welche auch in dieser Studie zum Einsatz kam, korrelierte bei MS Patienten (70% RRMS) besser mit der Lebensqualität als klassische Hochkontrast- und Niedrigkontrastsehtafeln.[37] Ein reduziertes Kontrastempfinden wurde bei Patienten nach Optikusneuritis[38], hinterer Glaskörperabhebungt[39], mit Myopia magna unter -12,0 Dioptrien (sowohl mit Brillengläsern wie auch mit Kontaktlinsen korriegiert)[40] und Parkinson Patienten gefunden. Bei Parkinson Patienten korrelierten das verminderte Kontrastsehen mit Schlaf- und kognitiven Störungen. Des Weiteren hatten die Patienten mit unterdurchschnittlicher Kontrastsehfunktion bei Diagnosestellung ein höheres Risiko einen Abfall der kognitiven Funktion zur erleiden sowie für visuelle Halluzinationen.[41] Das Niedrigkontrastsehen bzw. die Kontrastsensitivitätsfunktion ist damit besser als Verlaufsprädiktor geeignet als das im klinischen Alltag weitaus häufiger evaluierte Hochkontrastsehen. Eine häufigere Testung der Kontrastsensitivitätsfunktion in der klinischen Patientenversorgung könnte zu einer besseren Einschätzung des Leidensdrucks und bei Therapieentscheidungen helfen. Computergestützte Methoden zur Bestimmung der Kontrastsensitivitätsfunktion könnten die verstärkte Implementierung in den klinischen Alltag erleichtern.[14]

2.5 Literaturverzeichnis

1. Faissner, S., Plemel, J. R., Gold, R. & Yong, V. W. Progressive multiple sclerosis: from pathophysiology to therapeutic strategies. *Nat. Rev. Drug Discov.* **18**, 905–922 (2019).
2. Petzold, A. *et al.* Retinal layer segmentation in multiple sclerosis: a systematic review and meta-analysis. *Lancet Neurol.* **16**, 797–812 (2017).
3. Petzold, A. *et al.* Retinal asymmetry in multiple sclerosis. *Brain* **144**, 224–235 (2021).
4. Sotirchos, E. S. *et al.* Progressive Multiple Sclerosis Is Associated with Faster and Specific Retinal Layer Atrophy. *Ann. Neurol.* **87**, 885–896 (2020).
5. Saidha, S. *et al.* Relationships between retinal axonal and neuronal measures and global central nervous system pathology in multiple sclerosis. *Arch. Neurol.* **70**, 34–43 (2013).
6. Ko, F. *et al.* Association of Retinal Nerve Fiber Layer Thinning with Current and Future Cognitive Decline: A Study Using Optical Coherence Tomography. *JAMA Neurol.* **75**, 1198–1205 (2018).
7. Pisa, M. *et al.* Subclinical neurodegeneration in multiple sclerosis and neuromyelitis optica spectrum disorder revealed by optical coherence tomography. *Mult. Scler. J.* **26**, 1197–1206 (2020).
8. Klumbies, K. *et al.* Retinal Thickness Analysis in Progressive Multiple Sclerosis Patients Treated With Epigallocatechin Gallate: Optical Coherence Tomography Results From the SUPREMES Study. *Front. Neurol.* **12**, 1–9 (2021).
9. Michael Khalil, Charlotte E. Teunissen, Markus Otto, Fredrik Piehl, Maria Pia Sormani, Thomas Gattringer, Christian Barro, Ludwig Kappos, Manuel Comabella, Franz Fazekas, Axel Petzold, Kaj Blennow, H. Z. & J. K. Neurofilaments as biomarkers in neurological disorders. Nature Reviews Neurology | 10.1038/s41582-018-0058-z. (2018).
10. Barro, C. *et al.* Serum neurofilament as a predictor of disease worsening and brain and spinal cord atrophy in multiple sclerosis. *Brain* **141**, 2382–2391 (2018).
11. Bittner, S., Oh, J., Havrdová, E. K., Tintoré, M. & Zipp, F. The potential of serum neurofilament as biomarker for multiple sclerosis. *Brain* **144**, 2954–2963 (2021).
12. Jens Kuhle 1, Tatiana Plavina 2, Christian Barro 1, Giulio Disanto 3, Dipen Sangurdekar 2, Carol M Singh 2, Carl de Moor 2, Bob Engle 2, Bernd C Kieseier 2, Elizabeth Fisher 2, Ludwig Kappos 1, Richard A Rudick 2, J. G. 2. Neurofilament light levels are associated with long-term outcomes in multiple sclerosis. *Mult. Scler. J.* (2020) doi:10.1177/1352458519885613.
13. Lin, T. Y. *et al.* Increased Serum Neurofilament Light and Thin Ganglion Cell-Inner Plexiform Layer Are Additive Risk Factors for Disease Activity in Early Multiple Sclerosis. *Neurol. Neuroimmunol. neuroinflammation* **8**, 1–10 (2021).
14. Rosenkranz, S. C. *et al.* Validation of Computer-Adaptive Contrast Sensitivity as a Tool to Assess Visual Impairment in Multiple Sclerosis Patients. *Front. Neurosci.* **15**,

1–8 (2021).

15. Tewarie, P. *et al.* The OSCAR-IB consensus criteria for retinal OCT quality assessment. *PLoS One* **7**, 1–7 (2012).

16. Sullivan, E. V. & Pfefferbaum, A. Diffusion tensor imaging in normal aging and neuropsychiatric disorders. *Eur. J. Radiol.* **45**, 244–255 (2003).

17. Kaps, M. & Lamberson, W. R. Mixed models. *Biostatistics for animal science* 305–309 (2017) doi:10.1079/9781786390356.0305.

18. Nolan, R. C. *et al.* Optimal Inter-Eye Difference Thresholds in Retinal Nerve Fiber Layer Thickness for Predicting a Unilateral Optic Nerve Lesion in Multiple Sclerosis. **38**, 451–458 (2022).

19. Balk, L. J. *et al.* Timing of retinal neuronal and axonal loss in MS: a longitudinal OCT study. *J. Neurol.* **263**, 1323–1331 (2016).

20. Paul, F. *et al.* Optical coherence tomography in multiple sclerosis: A 3-year prospective multicenter study. *Ann. Clin. Transl. Neurol.* **8**, 2235–2251 (2021).

21. Gigengack, N. K. *et al.* Structure–function correlates of vision loss in neuromyelitis optica spectrum disorders. *Sci. Rep.* **12**, 1–11 (2022).

22. Costello, F. *et al.* Quantifying axonal loss after optic neuritis with optical coherence tomography. *Ann. Neurol.* **59**, 963–969 (2006).

23. Stellmann, J. *et al.* Pattern of gray matter volumes related to retinal thickness and its association with cognitive function in relapsing – remitting MS. 1–14 (2017) doi:10.1002/brb3.614.

24. Balcer, L. J. *et al.* New low-contrast vision charts: Reliability and test characteristics in patients with multiple sclerosis. *Mult. Scler.* **6**, 163–171 (2000).

25. Gabilondo, I. *et al.* Trans-synaptic axonal degeneration in the visual pathway in multiple sclerosis. *Ann. Neurol.* **75**, 98–107 (2014).

26. Khalil, M. *et al.* Serum neurofilament light levels in normal aging and their association with morphologic brain changes. *Nat. Commun.* **11**, 1–9 (2020).

27. Pascal Benkert PhD a †, Stephanie Meier MSc b †, Sabine Schaedelin MSc a, Ali Manouchehrinia PhD e, Özgür Yaldizli MD b, Aleksandra Maceski MSc b, Johanna Oechtering MD b, Lutz Achtnichts MD g, David Conen MD i, Tobias Derfuss MD b, Patrice H Lalive MD l, K. B. P. p…Chiara Z. Serum neurofilament light chain for individual prognostication of disease activity in people with multiple sclerosis. *Lancet Neurol.* (2022).

28. Williams, T., Zetterberg, H. & Chataway, J. Neurofilaments in progressive multiple sclerosis : a systematic review. *J. Neurol.* **268**, 3212–3222 (2021).

29. Modvig, S. *et al.* Cerebrospinal fluid neurofilament light chain levels predict visual outcome after optic neuritis. *Mult. Scler.* **22**, 590–598 (2016).

30. Liu, W. W. *et al.* Three-dimensional neuroretinal rim thickness and visual fields in glaucoma: A broken-stick model. *J. Glaucoma* **29**, 952–963 (2020).

31. Gadi Wollstein1, Larry Kagemann1, 2, Richard A Bilonick1, Hiroshi Ishikawa1, 2, L. S.,

Folio1, Michelle L Gabriele1, 2, Allison K Ungar1, Jay S Duker3, James G Fujimoto4, and J. & S Schuman1, 2, 5. Retinal nerve fibre layer and visual function loss in glaucoma: the tipping point. *Br. J. Ophthalmol.* (2012) doi:10.1136/bjo.2010.196907.

32. Alasil, T. *et al.* Correlation of retinal nerve fiber layer thickness and visual fields in glaucoma: A broken stick model. *Am. J. Ophthalmol.* **157**, 953-959.e2 (2014).

33. Havla, J. *et al.* Age-dependent favorable visual recovery despite significant retinal atrophy in pediatric MOGAD: how much retina do you really need to see well? *J. Neuroinflammation* **18**, 1–10 (2021).

34. Cormack, F. K., Tovee, M. & Ballard, C. Contrast sensitivity and visual acuity in patients with Alzheimer's disease. *Int. J. Geriatr. Psychiatry* **15**, 614–620 (2000).

35. Elliott, D. B., Hurst, M. A. & Weatherill, J. Comparing clinical tests of visual function in cataract with the patient's perceived visual disability. *Eye* **4**, 712–717 (1990).

36. Vingopoulos, F. *et al.* Measuring the contrast sensitivity function in non-neovascular and neovascular age-related macular degeneration: The quantitative contrast sensitivity function test. *J. Clin. Med.* **10**, (2021).

37. Dorr, M. & Heesen, C. Introducing a new method to assess vision : Computer-adaptive contrast-sensitivity testing predicts visual functioning better than charts in multiple sclerosis patients. (2015) doi:10.1177/2055217315596184.

38. Sanchez-Dalmau, B. *et al.* Early retinal atrophy predicts long-term visual impairment after acute optic neuritis. *Mult. Scler. J.* **24**, 1196–1204 (2018).

39. Garcia, G. A. *et al.* Degradation of Contrast Sensitivity Function Following Posterior Vitreous Detachment. *Am. J. Ophthalmol.* **172**, 7–12 (2016).

40. Liou, S., Chiu, C., Liou, S. & Chiu, C. Myopia and contrast sensitivity function. **3683**, (2009).

41. Hong, S. Bin *et al.* Contrast sensitivity impairment in drug-naïve Parkinson's disease patients associates with early cognitive decline. *Neurol. Sci.* **41**, 1837–1842 (2020).

3. Zusammenfassung

3.1 Deutsche Version

Wir führten eine Beobachtungsstudie mit 81 Patienten mit Primär Progredienter Multipler Sklerose (PPMS) durch, welche longitudinale Sehleistungsparameter, Messungen mithilfe der optischen Kohärenztomographie (OCT), Magnetresonanztomographie (MRT) und die Bestimmung des Serum Neurofilament Light Chains (sNfL) beinhaltete. Darüber hinaus erfolgte ein querschnittlicher Vergleich mit zwei Kohorten jeweils 52 gesunder Probanden. Ziel der Studie war es, Prädiktoren des klinischen Verlaufs der PPMS zu identifizieren. Diskutiert werden dafür die Atrophie retinaler Nervenschichten und die Konzentration des Proteins sNfL.

Im querschnittlichen Vergleich mit gesunden Probanden hatten PPMS Patienten verminderte Parameter der Kontrastsensitivitätsfunktion, eine dünnere Retinale Nervenfaserschicht (RNFL) und Ganglienzell-/Innere Plexiforme Schicht (GCIPL) sowie ein erhöhtes sNfL. Auch mit zunehmender Krankheitsdauer nahmen die RNFL, GCIPL und das totale Makulavolumen ab. Die Atrophie der retinalen Nervenschichten beeinflusste die Sehleistungsparameter in einem nicht-linearen Zusammenhang. Die Sehleitung blieb lange bis zu einem bestimmten Wendepunkt der retinalen Atrophie weitestgehend stabil, nach welchem ein deutlich steilerer Abstieg der Sehfunktion zu verzeichnen war. Die Fläche unter der logarithmierten Kontrastsensitivitätsfunktion zeigte von allen gemessenen Sehleistungsparametern den steilsten Abstieg und scheint somit ein sensitiverer Parameter für die Neurodegeneration bei PPMS zu sein.

3.2 Englische Version

Our observational study with 81 primary progressive multiple sclerosis (PPMS) patients includes a longitudinal assessment of the visual function, measurements performed with the optical coherence tomography (OCT), magnetic resonance imaging (MRI) and the evaluation of the serum neurofilament light chain protein (sNfL). Additionally, we performed a cross sectional comparison with two groups of healthy controls, each n=52. The purpose of the study was to identify predictors for clinical worsening of PPMS. As such potential predictors, we discuss the retinal layer atrophy and the concentration of sNfL.

In the cross sectional comparison with healthy controls, PPMS patients showed a lower contrast sensitivity function, thinner retinal nerve fiber layer (RNFL) and ganglion cell/inner plexiform layer (GCIPL) and total macula volume. There was a non-linear association between the visual function and retinal layer atrophy. Visual funcion was largely stable until an inflection point after which a notably steeper decline was observed. The area under the logarithmized contrast sensitivity function had the steepest decline of all measured visual function parameters and therefore, seems to be a more sensitive parameter for neurogedeneration in PPMS.

4. Erklärung des Eigenanteils

Der Schwerpunkt meines Eigenanteils an der Publikation liegt auf der Evaluation der OCT Aufnahmen und der Sehleistungsfunktion und erstreckt sich auf folgende Punkte:

- Datenmanagement, Prozessierung und Auswertung der OCTs inklusive semiautomatischer Segmentierung der OCT Aufnahmen und Prüfung der OSCAR-IB Kriterien
- statistische Datenauswertung- und Interpretation unter Supervision von PD Dr. Jan-Patrick Stellmann
- Erstellung von Graphiken zur Datenillustration
- Literaturrecherche und Verfassung der Publikationsschrift in Koautorenschaft mit Sina Rosenkranz
- Konzept und Analyseplan

5. Danksagung

Zunächst möchte ich mich herzlich bei meinem Doktorvater, PD Dr. Jan-Patrick Stellmann, für seine hervorragende Betreuung und Unterstützung bedanken. Trotz seines Umzugs nach Frankreich war er zu jeder Zeit erreichbar und stand mir mit kompetentem Rat und Hilfestellungen zur Seite. In jeder Phase des Promotionsprozesses begleitete er mich stets ruhig und verständnisvoll.

Mein Dank gilt Professor Dr. Christoph Heesen, Leiter der MS-Ambulanz des Universitätsklinikums Hamburg-Eppendorf, für die Ermöglichung der Durchführung der Studie.

Auch danke ich Dr. Sina Rosenkranz, der Co-Erstautorin der Publikation, für ihr Engagement und ihre Kollegialität.

Dem ganzen Arbeitsteam möchte ich für die freundliche Zusammenarbeit danken.

Ohne die Probanden, welche freiwillig an der Studie teilnahmen, sich die Mühe machten, unsere Ambulanz aufzusuchen und die Untersuchungen über sich ergehen ließen, wäre die Publikation nicht möglich gewesen. Ihnen gebührt ein großes Dankeschön.

Des Weiteren danke ich meiner Freundin und damaligen Mitbewohnerin, Alicia Pezzella.

Meinem Lebensgefährten, Óscar Sanz Mora, danke ich dafür mich immer wieder motiviert zu haben und für seine emotionale und kulinarische Unterstützung.

Zu besonderem Dank bin ich meinen Eltern und Großeltern verpflichtet, die mir das Studium finanziell ermöglichten und mich in allen Lebenslagen unterstützten und ermutigten.

9. Lebenslauf

Der Lebenslauf wurde aus datenschutzrechtlichen Gründen entfernt.

10. Eidesstattliche Versicherung

Ich versichere ausdrücklich, dass ich die Arbeit selbständig und ohne fremde Hilfe verfasst, andere als die von mir angegebenen Quellen und Hilfsmittel nicht benutzt und die aus den benutzten Werken wörtlich oder inhaltlich entnommenen Stellen einzeln nach Ausgabe (Auflage und Jahr des Erscheinens), Band und Seite des benutzten Werkes kenntlich gemacht habe.

Ferner versichere ich, dass ich die Dissertation bisher nicht einem Fachvertreter an einer anderen Hochschule zur Überprüfung vorgelegt oder mich anderweitig um Zulassung zur Promotion beworben habe.

Ich erkläre mich einverstanden, dass meine Dissertation vom Dekanat der Medizinischen Fakultät mit einer gängigen Software zur Erkennung von Plagiaten überprüft werden kann.

Unterschrift: ..... Lilija Gutmann.....